

Experimental Proposal

Proposal for a Prompt Neutrino  
Experiment at Fermilab

B.P. Roe, C.T. Coffin, H.R. Gustafson, L.W. Jones, M.J. Longo, T.J. Roberts

University of Michigan  
Ann Arbor, Michigan 48109

and

U. Camerini, M. Duffy, W.S. Fry, R.J. Loveless, D.D. Reader, T. Trinko

University of Wisconsin  
Madison, Wisconsin 53706

and

T.Y. Ling

Ohio State University  
Columbus, Ohio 43210

September, 1978

66, 292

Proposal for a Prompt Neutrino

Experiment at Fermilab

C.T. Coffin, H.R. Gustafson, L.W. Jones, M.J. Longo, T.J. Roberts, B.P. Roe  
University of Michigan  
Ann Arbor, Michigan 48109

and

U. Camerini, M. Duffy, W.S. Fry, R.J. Loveless, D.D. Reader, T. Trinko  
University of Wisconsin  
Madison, Wisconsin 53706

and

T.Y. Ling  
Ohio State University  
Columbus, Ohio 43210

SUMMARY

In the present experiment we plan to measure prompt neutrino production as a function of proton beam energy and atomic number of target. With the apparatus to be described below we will be able to measure the angular distribution of prompt neutrinos to about 25 mr and the energy distribution for these neutrinos. In order to insure that we are indeed seeing prompt neutrinos, data must be collected at various target densities and (depending on the setup) intensities on target for constant beam line intensity. Assuming runs at 3 proton energies, 3 values of A, 3 densities and 3 intensities we need about 9 runs, requiring a total of  $\sim 1-2 \times 10^{17}$  protons on a target located 100-200 ft from the detector. This short target-detector separation permitting a high event rate for modest beam and detector mass, and permitting a large solid angle acceptance is a crucial feature of this proposal.

The detector we will use is a lead-scintillator calorimeter followed by an iron toroidal muon spectrometer. PWC planes with  $\pm 1$  cm resolution will be placed between calorimeter modules and behind the magnets for track definition. Most of the equipment needed exists now. We need a beam intensity of about  $10^{12}$  ppp. With this intensity we will get an event with visible energy greater than 20 GeV every 10-15 pulses using the CERN prompt neutrino results and the results of a preliminary experiment we have done in spring 1978. (This corresponds to  $\sigma_{D \text{ pair}} \sim 30-60$  pb depending on the model. At  $\sim 10^{12}$  ppp we can vary the A of the target up to tungsten, something difficult to do in experiments requiring higher beam intensity.

## INTRODUCTION

We propose a beam dump experiment at Fermilab to study the production of prompt neutrinos. We have been stimulated by the CERN beam dump results, by the interesting observations on direct muon production by E379, E436, and E439 at Fermilab, and by the so-far negative results of charmed meson searches in hadron production experiments.

In the present experiment we plan to measure prompt neutrino production as a function of proton beam energy and atomic number of target. With the apparatus to be described below we will be able to measure the angular distribution of prompt neutrinos to  $> 40$  mr and the energy distribution and lepton number for these neutrinos. In order to insure that we are indeed seeing prompt neutrinos, data must be collected at various target densities and (depending on the setup) intensities on target for constant beam line intensity. Assuming runs at 3 proton energies, 3 values of  $A$ , 3 densities and 3 intensities we need about 9 runs requiring a total of  $\sim 1-2 \times 10^{17}$  protons on target.

As a consequence of the earlier results mentioned above, the Michigan members of this group mounted a modest test in the M2 beam line parasitic to E439. The analysis of this short run is now complete; there is a small but positive signal for neutrino-induced events in this test, and the interpretation of these data together with the CERN data reinforces the interpretation that the observed neutrinos are from a prompt process characterized by large  $p_{\perp}$ . The report is included as Appendix A of this proposal. We believe that the experience gained in this test is a valuable asset in designing a more significant experiment, both in estimating event rates and in anticipating pitfalls and problems.

The detector we will use is a lead-scintillator calorimeter followed by an iron toroidal muon spectrometer. Most of the equipment needed exists now. We need a beam intensity of about  $10^{12}$  ppp. With this intensity we will get an event with visible energy greater than 20 GeV every 10 pulses using the CERN results and the results of our preliminary experiment. (This corresponds to  $\sigma_{D \text{ pair}} \sim 30-60 \mu\text{b}$  depending on the model). At  $\sim 10^{12}$  ppp we can vary the A of the target up to tungsten, something difficult to do in experiments requiring higher beam intensity.

There are several problems with which a prompt neutrino experiment must cope. The prompt muon flux from a beam dump target is very high, even through 10 m of steel. It is essential that the magnetization of iron in or beyond the beam dump be parallel to the major transverse dimension of the detector, as the muon flux is seen to increase dramatically off the median plane (defined to include B). In this context a dump target followed by a solid iron magnetic spectrometer with B horizontal as in E439 is quite suitable.

In our preliminary experiment we noted a neutrino event background of the order of 1/2 the prompt neutrino signal due to upstream neutrino sources in M2. For the proposed experiment we must reduce the background to a very low level. It is important therefore that the beam incident on the dump target be very clean, with care paid to collimator scraping, beam line vacuum, and halo effects. It is also important to study such background with direct measurements of beam line-generated muons and other background.

In order to appraise the ratio of beam dump prompt neutrinos to  $\pi/K$  neutrinos, it would be desirable to vary the target density keeping A constant (for example with an accordion target as in prompt muon production experiments).

Cosmic ray-induced energetic events may mimic neutrino events on the basis of pulse height alone. Position and direction information on each event as well as good timing data will improve cosmic ray rejection; nevertheless shielding and anticoincidence counters will be employed to as great an extent as feasible.

#### EXPERIMENTAL APPARATUS AND BEAM

a. Detector. We propose using the lead-scintillator shower detectors built for E-310 as the calorimeter. This detector can be rearranged to give a 5' x 10' cross-section detector which is  $3000 \text{ gm/cm}^2$  thick. This detector will be placed off center as shown in Figure 1. It is composed of a lead plate-liquid scintillator sandwich. The details of the response of one module of this detector as measured by E-310 are given in Appendix B. Planes of proportional tubes will be inserted between each of the 30 modules to give position information on the shower. This will also allow us to measure the direction of the shower and will be a powerful aid in reducing non-beam background. The apparatus will have an ability to measure relative rates of  $\nu_\mu$ ,  $\bar{\nu}_\mu$  and  $(\nu_e + \bar{\nu}_e)$  charged current events. The electro-magnetic component of the showers will die out much more quickly than the hadronic. (The radiation length in Pb is 0.56 cm while the nuclear interaction length is 18.5 cm.) Individual muons above about 4 GeV will be seen by their penetration in the detector. PWC planes would be placed between each pair of detector modules so as to give muon track coordinates as well as Hadron and EM cascade positions. The required resolution is modest, and proportional chamber planes made of extruded aluminum stock with rectangular apertures  $1/2 \times 3/4$  inches will be used. The track information thus available will permit identification of incident muons and hence aid in the anticoincidence rejection. Although the measurement of the prompt neutrinos can be

accomplished with the calorimeter alone, the experiment is enhanced by the addition of a solid iron muon spectrometer. Measurement of the sign of the muon will allow separation of  $\nu_{\mu}$  events from  $\bar{\nu}_{\mu}$  events. The momentum measurement will increase the energy resolution for muon charged current events.

The spectrometer would consist of two solid iron magnets each 1.2 m in length and about 4 m in transverse dimensions. Based on our experience with the similar magnets used in E1A, and E439 we estimate a field strength  $> 1.8T$ . Four planes of proportional tubes similar to those installed in the calorimeter would be used to measure the trajectory. The accuracy for point measurement would be  $\sim \pm 1$  cm. The ratio of  $p_{\perp}(\text{ms})$  to  $p_{\perp}(\text{bend})$  is 15%.

b. Anti-coincidence. A plane of anti-coincidence counters will cover the front face of the detector. We will be careful to limit their extent in the vertical direction. This will be discussed in detail in the background section. The calorimeter should be shielded by a concrete house.

c. Target and beam dump. In our preliminary experiment (report enclosed) the beam dump had 5.5 m of 2.1 T field. As we discuss in the background section we need about 8 m of 2.1 T horizontal field for this experiment giving a  $p_{\perp}$  of 5 GeV/c. This can be a solid iron magnet of modest dimensions. An area of 12"(h) x 15"(v) would be sufficient for the region of high field. There should be a total of at least a 13 m length of iron or equivalent in the dump. (The last 1 or 2 m of iron equivalent could be shielding blocks.)

nb. The beam dump design is a crucial part of this experiment. However, we expect that there may well be a series of beam dump experiments especially as the accelerator energy increases.

The target design must also be carefully engineered. There must be a mechanism for moving different targets into place and accomodating long targets of low density. The target will be about 100-200 ft from the calorimeter. This will be negociable depending on the area.

We would expect to work together with Fermilab personnel in developing plans for the construction of the beam dump and target facilities.

d. Beam Line. Special care must be taken to avoid scraping. "Neck down regions" of small diameter vacuum pipes are to be avoided. Shielding must be placed between potential trouble spots and the calorimeter as close as possible to the problem spots (to avoid meson decay). Various detectors would be used to monitor backgrounds.

e. Area. This experiment could go into any of several places. In the meson lab, M1, or M2 could be used. In the proton area p- center is an attractive site depending on details of scheduling. We will be discussing placement possibilities with lab personnel shortly.

#### EVENT RATES

We assume a 400 GeV proton beam of  $10^{12}$  pp on a tungsten target and for the moment neglect dead time. From the results of our preliminary experiment we then estimate 1 event every 10 pulses resulting in  $> 20$  GeV deposited in the detector. Using the CERN BEBC rate we estimate 1 per 15 pulses.

If there are 5000 pulses on an average day then this is 500 events/day. To make 9 runs with  $\sim 1000$  events/run for high E and high A is then 20 days with no dead time. We therefore request  $1 - 2 \times 10^{17}$  protons on target. If we were in, for example, the M1 beam, we could get a clean pion beam of  $\sim 10^{10}$   $\pi$ /pulse. Then, (with a sharp bend of  $\sim 20$  mr just before the target) we

might be able to compare and p and  $\pi$  production of prompt neutrinos.

#### BACKGROUND AND DISCUSSION

The previous experiment enabled us to get a realistic idea of the background and problems facing us.

In that experiment dead time was a very serious problem. In fact the live time on the data runs was only 22% for a beam intensity of  $1.5 \times 10^{11}$  ppp on target. The proposed apparatus subtends about the same solid angle as in the previous experiment. We believe, however, that the problem can be significantly reduced for the present experiment.

Figure 2 illustrates the radiation level measured at different positions around the calorimeter in the preliminary experiment. (Appendix A) Comparison with the measured flux of through going muons indicates that the background is predominately muons. The most important thing to note is the large vertical variation. The dump magnet has provided a strong vertical minimum at the center of the calorimeter. The distance between the target and detector (50 m) is arranged so that the calorimeter subtends about the same angle vertically as in the preliminary experiment. Unfortunately, in the preliminary experiment it was necessary to extend counters down to the floor and up an equal amount. As can be seen this increased the veto counting rate by close to an order of magnitude. The present design will protect the calorimeter with counters but not over extend them in the vertical direction.

A further factor is gained by increasing the  $p_1$  given to muons by the dump magnet from the value used in the preliminary experiment. From the steep vertical flux variation it is seen that the background is a sharp function

of the amount of bending in the dump. A 250 GeV muon will be bent by about 1 meter before reaching the calorimeter with the new arrangement. The two improvements together should reduce the dead time to a tolerable value. Finally, we would segment the veto counter and thus further reduce the dead time if it were necessary. In summary, it is clear that an improved dump is needed but, as indicated above, we believe it would be used in several experiments and be a cost effective facility.

In our preliminary experiment we found we were able to reduce the total background to about one-half the signal level. In the present design the ability to distinguish position and direction of the shower is expected to reduce the background substantially. We believe that by careful beam design to reduce scraping, shielding trouble spots, having a better anti-system and shielding around the calorimeter we can reduce the background to quite low levels. We expect to measure the cross-section for the production of prompt neutrinos to a precision of 10-20%.

TENTATIVE EQUIPMENT LIST:

	Experimenter	FL (existing)	FL (requiring new expenditures)
Beam, Target, Beam Dump			X
Halo Monitors	X		
Veto Hodoscope	X		
350 PM tubes	X		
HV and distribution for 350 PM		45K	
340 ADC readout		20K	
5000 wires PW tube system HV	X		
Readout for 5000 PW tubes	X		
12" x 6' x 12' steel shield			230 tons
2" x 6' x 12' steel shield			~ 50K
2 solid iron magnets			
Power Supply for solid iron magnet		X	
PDP 11 standard operating configuration		X	
Fast logic electronics		~ 85K	

Caveat: The detailed specific configuration depends upon the location. Once the location is determined detailed cost estimates can be prepared.

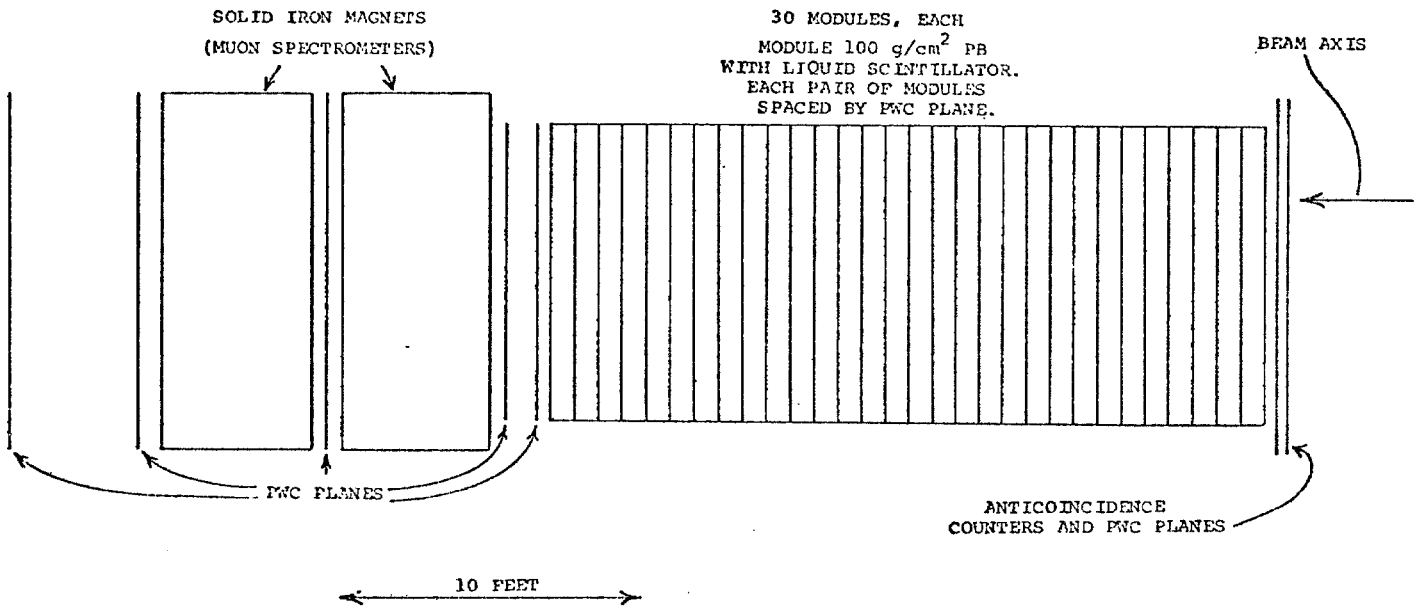


FIGURE 1

DETECTOR CONFIGURATION  
NEUTRINO BEAM DUMP  
EXPERIMENT

B.P. ROE ET AL.

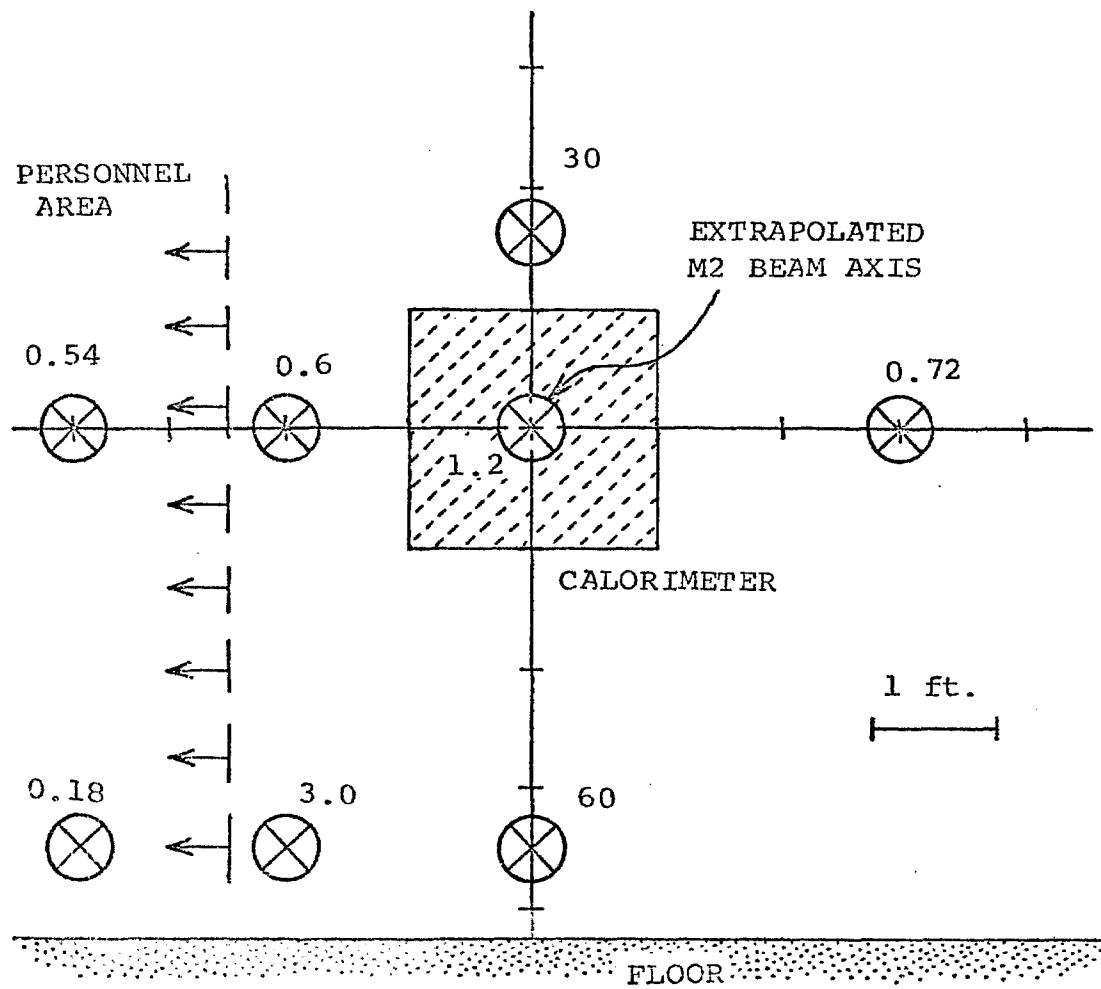


FIGURE 2

RADIATION LEVEL (MUONS) AT NEUTRINO  
 TEST AREA BEHIND E439.  
 LEVELS ARE IN mR PER HOUR WITH  
 $\sim 10^{11}$  PROTONS PER PULSE ON E439 TARGET.

A Prompt Neutrino Measurement\*

B.P. Roe, H.R. Gustafson, K.J. Heller, L.W. Jones,  
and M.J. Longo

University of Michigan  
Department of Physics  
Ann Arbor, MI 48109

September, 1978

ABSTRACT

A test has been made to explore the possibility of beam dump neutrino experiments with short target-detector separations and modest detectors. Results have given a positive neutrino signal which is interpreted in the context of various charmed-meson production models. A limit to the lifetime and mass of the axion is also a byproduct of this test.

\*Supported by the U.S. National Science Foundation and the Department of Energy

## I. INTRODUCTION

A test experiment has been performed parasitically in the M2 diffracted proton beam of the meson lab at Fermilab. A dimuon experiment, E439,<sup>1</sup> targeted protons on a thick tungsten target with was followed by a 5.5 m solid iron magnet assembly magnetized to 2.1 T (B horizontal). The neutrino detector was a 4-ton iron calorimeter<sup>2</sup> located 22 m from the tungsten target behind an additional 5.4 m of steel, as indicated in Figure 1.

Results from beam dump experiments at CERN<sup>3</sup> have indicated a source of prompt neutrinos, and D-pair production has been suggested as the mechanism. If the area of the neutrino beam is comparable to the detector area and the target-to-detector distance is fixed (as is the case in standard neutrino experiments), neutrino detection rates are related only to total detector fiducial mass. However if prompt neutrinos exist and are produced with a rather large characteristic  $p_{\perp}$  (e.g.  $\approx 1$  GeV/c) but short target-to-detector distances are used, then the event rate will be proportional to detector mass per unit area times solid angle, or mass divided by target-detector separation squared. In this experiment a 4 ton detector 22 m from the target subtended  $\pm 14$  mr from the target (corres. to a 35 GeV  $\nu$  of  $p_{\perp} \sim 0.5$  GeV/c) whereas the CERN detectors were about 800 m from the target, and subtended  $\pm 2$  mr. Not only is

a larger fraction of direct neutrinos thus sampled, but the background due to  $\pi$  and k decay neutrinos (which fall into a narrower solid angle) is effectively suppressed.

This experiment was implemented toward the end of E439 running so that the running time corresponded to only about  $2 \times 10^{15}$  protons on target, and this was further significantly reduced by deadtime. Nevertheless a positive signal was obtained.

## II. EXPERIMENTAL DETAIL

Even behind the 10.9 m of iron the muon flux was very high; a 30 x 30 cm<sup>2</sup> scintillator telescope straddling the calorimeter on the beam axis recorded 5000 $\mu$  per 10<sup>11</sup> protons on target.<sup>4</sup> As about 0.2% of energetic  $\mu$ 's produced an interaction in the calorimeter corresponding to  $\approx$  20 GeV energy release, it was necessary to shield the front face of the calorimeter with anticoincidence counters. Another source of false signal could be cosmic ray events - hadrons or air showers-from above. One 60 x 120 cm<sup>2</sup> anticoincidence scintillator was accordingly put on top of the calorimeter. The experiment was located at the end of the Meson Detector Building with no overhead shielding. In order to reduce the calorimeter albedo from desired events from triggering this top counter, 5 cm of borated polyethylene were placed between the calorimeter and this counter.

The calorimeter consisted to 30 steel plates each 61 cm square and 3.9 cm thick with 0.64 cm scintillator between. The scintillator light was piped to four phototubes (Figure 2) which permitted left-right and front-back signal comparisons. Calibration in a test beam gave a calorimeter resolution  $\sigma = (73/\sqrt{E})\%$  for hadrons of 20-40 GeV. Cherenkov pulses from the phototube light pipes were a possible source of concern;

anticoincidence shielding and the requirement of comparable pulses from phototubes on opposite sides should have effectively reduced this problem.

The outputs from the seven anticoincidence counters were fed to LeCroy 621AL discriminators, run in the burst-guard mode, and the discriminators' outputs summed together. Their rate was about  $5 \times 10^6$  per pulse during the longest data run. During this period the system live time (i.e. fraction of the beam pulse gate not vetoed by the anticoincidence system) was only 22%. The calorimeter threshold was set at about 3.5 times the most probable muon pulse height, or about 10 GeV, based on earlier calibrations. With the anticoincidence requirement, the "event" rate was about one trigger per  $2 \times 10^{12}$  protons on target, still about 20 to 50 times the expected neutrino event rate. With a 20 GeV cut on the data, most events still appeared spurious. A variety of strategies were used to reduce this rate to permit extraction of meaningful data. These are enumerated below:

A. Right-left signals: since the scintillators alternate, pulse heights from the right and left side phototubes should be comparable. Reasonable bounds of  $\pm 2\sigma$  were set for the limits of the right:left pulse height ratio. These bounds corresponded to a variation in the pulse height ratio of  $2.92/\sqrt{E}$  (GeV), and agreed with scatter-plot distributions from runs with the anti-coincidence counters off, i.e.

muon initiated events. Muons travelling along the light pipes could mimic an energetic hadron cascade except for this criterion.

B. Event Timing: the accelerator r.f. signal was timed with muons through the system and the arrival time of the pulses in each of the four calorimeter phototubes was digitized relative to the r.f. Good neutrino candidates were then required to have the same time coincidence with the r.f. as muon-initiated cascades of comparable energy, which were observed to lie within a band of 4 ns width.

C. Time difference between left and right calorimeter phototubes: the time differences between phototubes vs. the summed output of those two tubes, studied separately for the front and back halves of the calorimeter provided an additional timing constraint. This difference was required to lie within bounds of 6 ns (low E) to 4 ns (high E) for the muon runs. This time spread was further narrowed by plotting the right-left time difference vs.  $\frac{\text{pulse ht}(\text{right}) - \text{pulse ht}(\text{left})}{\text{pulse ht}(\text{right}) + \text{pulse ht}(\text{left})}$ .

D. The analogue signals from the anti-counters were digitized: this permitted ex-post-facto examination of the anticoincidence efficiency. From muon and anti-coincidence-off runs, pulse height distributions corresponding to minimum

ionizing particles in each counter were determined. The maximum permitted pulse height was about  $1/5 - 1/10$  the mean muon signal.

The ADC system digitized pulse area within the determined gate, whereas the anticoincidence discriminator responded to pulse height. It is thus possible for the long tail of a previous large pulse to be recorded as a large ADC pulse height while not triggering the anticoincidence discriminator. The conservative approach is to set rigid maximum allowable ADC levels for each of the seven veto counters; these result in one set of values in Tables I, II, and III. An upper limit on the true neutrino signal is obtained by ignoring the veto ADC signals and assuming that the electronics functioned ideally. These values are also noted in the tables.

The fiducial volume of the calorimeter is not certain; it is probable that vertices within 2 inches of the side edges of the calorimeter are recorded at significantly lower efficiencies, hence we take the area to be  $2500 \text{ cm}^2$  ( $50 \times 50 \text{ cm}$ ). The depth will be less than the  $900 \text{ g/cm}^2$  again because cascades close to the back of the calorimeter will be detected inefficiently. Some measure of this effect may be learned from the ratio of events detected in the front alone to those detected in the back alone on muon (no anticoincidence) runs. From such data it appears that, of 64 events,

25 appear in the front, 31 in the back, and 8 with comparable signals in both front and back. The front includes  $360 \text{ g/cm}^2$  and the back  $540 \text{ g/cm}^2$  of iron. If the "front" plus "front plus back" events represent muon events with vertices in the front  $360 \text{ g/cm}^2$ , then the effective mass of the "back" is  $(31/33) \times 360$  or  $340 \text{ g/cm}^2$ . This suggests an effective total fiducial thickness for the calorimeter of  $\sim 700 \text{ g/cm}^2$ . The overall effective mass would then be about 1.75 metric tons.

Because of the anticoincidence counter which lay over the calorimeter to veto cosmic ray air showers, there was some probability that a neutrino event in the calorimeter would produce a scattered particle into this counter and veto itself. This was evaluated by looking both at the fraction of muon initiated events in which this counter fired, and by operating the system in a parasitic hadron beam and observing the fraction of events in which this counter fired.

This fraction ranged from 32% for 20 GeV events to 44% for 40 GeV hadrons. A value of 30% was obtained from the muon-initiated events (peaked at lower energy). The hadron data for this fraction fit an empirical function

$$f_i = 0.32 + 0.006 (E_i - 20),$$

so that a corrected number of events can be obtained by scaling with a factor

$$K = \frac{1}{N} \sum_{i=1}^N \frac{1}{1 - f_i} .$$

### III. RESULTS

Data were taken under four conditions: (1) high intensity on E-439 (data run), with about  $1.5 \times 10^{11}$  protons per pulse (runs 54 and 58); (2) low intensity on E-439 target, at about 10% the data run intensity, or about  $1.3 \times 10^{10}$  protons per pulse (runs 69 and 71); (3) very low intensity, less than  $10^9$  protons per pulse (runs 74 through 79); and (4) cosmic rays (accelerator off; run 104). During (1), (2), and (3) the beam on the Meson area target was similar; about  $2 \times 10^{12}$  per pulse.

The primary data from the high intensity run (1) contained 8 events of over 20 GeV if all cuts are applied, or 14 events if the digitized veto counter levels are ignored. The energies of these events are tallied in Table I.

The data could be normalized in different ways; either to protons on target or to upstream background, as monitored by a scintillation counter on the mezzanine of the Meson Detector Building. The cosmic ray rate provides a reasonably certain (and statistically sound) background which may be subtracted from each of the data sets. It corresponds to about 10% of the high-intensity event rate.

The two lower-intensity runs provide somewhat contradictory data, although the statistics are sufficiently modest to render an apparent contradiction rather insignificant. The low intensity runs may be used either to represent the background due to protons on the meson target (i.e., invariant per unit of time or per pulse) or to the effect

of upstream beam scrapping and collimation in the M2 beam line, as measured by the mezzanine scintillation counter. The latter seems both more plausible and more self consistent. In either case, a background of  $\pi^-$  and k-decay neutrinos is shown to be present. The measured muon flux per pulse was actually about 1 1/2 times greater during the low intensity runs 69 and 71 than during the data runs 54 and 58, although the muon rates correlated rather well with rates in the mezzanine counter. On the other hand, there were over twice as many neutrino events per muon in the data runs as in the low intensity runs. Thus most of the observed muons as well as  $\sim 40\%$  of the neutrino events may be from upstream beam scrapping. The proton beam direction at the Meson Area target is 27 mr displaced from the line of sight distance from our detector. However the first bends in the M2 beam line would effectively channel some  $\pi^+$  and  $K^+$  along trajectories directed more nearly toward our detector.

From Table II it is seen that 8 events survive all cut criteria from the high-intensity data run; if the ADC data from the veto counter are ignored, 14 events survive. In Table III the effective number of beam dump events, either including or discounting the veto ADC data, are corrected for cosmic ray events and then for background assuming either that the mezzanine counter represents the true background rate or that the number of pulses (proportional to protons on the meson area target) represents appropriate background. On grounds of both plausibility and self

consistency, it was subjectively decided to weight the corrected number of events 3:1 in favor of the mezzanine-corrected results. When averaged over both sets of lower-intensity runs and corrected for the self-veto effect, a pair of best-guessed net numbers of beam dump neutrino events are obtained: 6.2 (including veto ADC's) and 13.8 (ignoring veto ADC's). With the obvious uncertainties reflected by the diverse entries in Table III, we will taken  $10 \pm 5$  as the best estimate of true neutrino events.

#### IV. ERRORS

The scattered entries in Table III represent the uncertainties in background and true beam-dump neutrino event rate, and emphasize both the need for careful beam preparation (to avoid upstream sources of  $\pi^-$  and k-decay neutrinos) and of careful measurements to appraise it. The best we can say from Table III is that our true signal appears to be  $10 \pm 5$  events. Various sources of error besides the background subtraction and veto ADC uncertainty (both adequately reflected in Table III) remain.

The fiducial mass of the calorimeter is uncertain to  $\pm 100 \text{ g cm}^{-2}$ , or  $\pm 14\%$  in depth, and  $\pm 2.5 \text{ cm}$  in radius, or  $\pm 22\%$  in area (although this is less significant in rates due to the radial fall-off in neutrino flux). Overall, the effective, radially-weighted fiducial mass is uncertain by  $\pm \sim 30\%$ .

The absolute calibration of the calorimeter is uncertain by  $\pm \sim 15\%$ , due to uncertainty of the muon energy and lack of a capability for hadron calibration at the time. In view of the fall off in event numbers with energy (4 events out of 14 with  $E = 20$  or  $21 \text{ GeV}$ ) this reflects as a  $\pm 30\%$  uncertainty in rate.

The various timing cuts are more certain, and very few events failed inclusion due to a "near miss" on timing. Likewise the cut on the ratio of pulse heights from the

two halves of the calorimeter. Nevertheless, there is no less than a  $\pm 15\%$  uncertainty due to the cumulative uncertainty of these criteria.

All of these effects taken together add up to a 45% uncertainty in the results of Table III. They do not, however, modify the evidence for a positive beam-dump signal.

V. INTERPRETATION

The number of detected neutrino events  $N_\nu$  may be expressed in terms of the number of incident protons  $N_p$  and the appropriate cross sections, solid angles, and efficiency factors as:

$$N_\nu = N_p \left\{ \frac{\sigma_\nu(NN)}{\sigma_I(NN)} F(N,W) \right\} \left\{ \rho \ell \sigma(E) G(E) \right\} \left\{ \Delta\Omega(M.C.) \right\} \quad (1)$$

In order to interpret direct neutrino production in terms of a specific model, it was assumed that all neutrinos come from D-decay, and that the branching ratio for semi-leptonic D-decay is 20%,<sup>5</sup> so that

$$\sigma_\nu(NN) = 0.4\sigma_D(NN) \quad (2)$$

where  $\sigma_D(NN)$  is the production cross section for D pairs in nucleon-nucleon collisions. (If D's are always produced singly, the appropriate D production cross section is twice  $\sigma_D(NN)$  defined here.)

Since the E-439 target is Heavimet (tungsten), it is necessary to interpret production processes in W in terms of elemental NN processes. As it appears that production of  $\psi$ 's, direct  $\mu$ 's, and large  $p_\perp$  mesons is proportional to  $\sim A^{1.0}$ , it is reasonable to make the same assumption for direct neutrino production. It is shown in Ref. 4 that

$$\frac{\sigma_\nu(NW)}{\sigma_I(NW)} = \left[ \frac{A \sigma_I(NN)}{\sigma_I(NW)} \right] \frac{\sigma_\nu(NN)}{\sigma_I(NN)}$$

where  $\sigma_I$ 's are NN and NW inelastic cross sections. For W the factor in brackets is 3.6. Because nucleons suffering inelastic interactions may be only somewhat degraded and may make subsequent nuclear interactions in the beam dump target there is a further enhancement due to cascading of  $\sim 12\%$ . Thus overall, a factor of 4 enhancement in the neutrino production is realized over that for a thin, hydrogen target. The factor  $F(N,W)$  is therefore taken as 4 in Eq. 1. The 12% enhancement factor is based on Drell-Yan processes with  $m \geq 7$  GeV, and does not include processes initiated by secondary pions. To the extent that the more copious lower energy pions are important in D production,  $F(N,W) = 4$  is an underestimate, and our deduced cross sections are corresponding overestimates.

The value for  $\rho l$  for the  $700 \text{ g cm}^{-2}$  (fiducial length) calorimeter is  $4.2 \times 10^{26} \text{ cm}^{-2}$ .  $\sigma(E)$  is the neutrino interaction cross section taken as

$$\sigma_{\nu}(E) = 0.6 E(\text{GeV}) \times 10^{-38} \text{ cm}^2,$$

$$\sigma_{\bar{\nu}}(E) = 0.25 E(\text{GeV}) \times 10^{-38} \text{ cm}^2,$$

where equal numbers of neutrinos and antineutrinos are assumed. The interaction cross section was further scaled by 1.32 to include neutral current events, so that  $\sigma(E)$  was taken as  $0.55E \times 10^{-38} \text{ cm}^2$ , with E in GeV. The function  $G(E)$  is the probability of detecting a  $\nu$  or  $\bar{\nu}$  of energy E in the calorimeter with a threshold set to 20 GeV. This is derived by folding the calorimeter resolution function with the calculated hadronic plus electro-magnetic products

of the neutrino interactions (assuming equal numbers of  $\nu$  and  $\bar{\nu}$ ). This distribution is sketched in Figure 3 for 40 GeV neutrinos. For this example,  $G(40) \approx 0.7$ .

The fraction  $\Delta\Omega(\text{M.C.})$  of produced neutrinos which fall into the solid angle subtended by the calorimeter, assumed to be  $50 \times 50 \text{ cm}^2$ , was calculated assuming that all came from D decays:  $D \rightarrow K + \ell + \nu$  or  $K^* + \ell + \nu$  using the observed  $\ell$  spectrum. A sample of 30,000 events was run through a Monte Carlo program for each of several assumed D production models. The results of these calculations are tabulated in Table IV. From the observed neutrino events, the resulting calculated D-production cross sections are also tabulated for the different production models. We have also compared our results with the CERN BEBC 0 mr and 15 mr observations, considering only the electron neutrino events. The CERN beam dump target was copper, for which the factor  $A\sigma_{\text{NN}}/\sigma_{\text{NA}} = 2.54$ . Including 12% for cascading, a factor of 2.8 is applied to the CERN 0 mr data to determine the cross section values of Table IV. The corresponding figure for the 15 mr data where a Be target was used is 1.67. The assumptions of the various D-production models are spelled out below.

Model I

$$p_{\perp} \text{ dependence} \propto e^{-6m_{\perp}} dp_{\perp}^2,$$

$$m_{\perp}^2 = p_{\perp}^2 + m_D^2,$$

$y_{\text{cm}}$  chosen uniform from  $-y_{\text{lim}}$  to  $+y_{\text{lim}}$ .

Model II<sup>3a</sup>

$$p_{\perp} \text{ dependence} \propto e^{-1.75p_{\perp}} dp_{\perp},$$

$$x \text{ dependence} \propto e^{-10|x|} dx, \quad x = \frac{p_{\parallel} \text{ cm}}{p_{\parallel} \text{ max}}.$$

This model has been used by Lauterbach<sup>6</sup>. He argues this is a fit to  $\psi$  production. Using this form and examining muon polarization data,<sup>7</sup> he sets a limit of  $\mu b$  on D production by 400 GeV p.

Since most experimenters find a different  $p_{\perp}$  dependence than that used by Lauterbach ( $\sim e^{-1.75p_{\perp}} dp_{\perp}^2$  rather than  $e^{-1.75p_{\perp}} dp_{\perp}$ ) we have tried the  $x$  dependence of his model and  $e^{-1.75p_{\perp}} dp_{\perp}^2$  for transverse momentum. This is Model IIb. Results for IIa and IIb are shown in Table IV.

Model IIIa<sup>7,8</sup>

$$E \frac{d^3\sigma}{dp^3} = \beta (1 - |x|)^4 e^{-1.6p_{\perp}},$$

This model is the result of fits to  $J/\psi$  production as indicated by experimenters of Refs. 7 and 8. We have tried modifying this by using  $e^{-2.2p_{\perp}}$  (Model IIIb). Results for Models IIIa and IIIb are shown in Table III also.

Model IV<sup>9</sup>

$$\frac{d^2\sigma}{dx dp_{\perp}^2} = \beta e^{-9.7x - 2.2p_{\perp}}, \quad x = p_{\text{lab}}/p_{\text{beam}}$$

This model is the result of another  $J/\psi$  experiment. The results are again shown in Table IV.

The most sensitive published search for D's from hadronic interactions by Ditzler et al.<sup>10</sup> determined 95% c.l. upper limit cross sections for  $K^{-}\pi^{+}$  ( $K^{+}\pi^{-}$ ) production at the  $D^0$  mass. With  $d\sigma/dp_{\perp}^2 \propto e^{-1.6p_{\perp}}$ , they determined  $B d\sigma/dy < 360$  nb (290 nb) at  $y = -0.4$  for  $D^0 \rightarrow K^{-}\pi^{+}$  ( $\overline{D^0} \rightarrow K^{+}\pi^{-}$ ). If D production is flat in  $d\sigma/dy$  over  $-1.5 < y < +1.5$  (equivalent to a bastardization of our

models Ib and IIIa), these results scale to an upper limit for  $B\sigma$  three times the values quoted. If further, the now-known branching ratio for  $D^0 \rightarrow K^- \pi^+$  of  $1.8 \pm 0.5\%$  is included, we have  $\sigma(D^0) < 48-60 \mu\text{b}$  per nucleon. If  $\sigma(D^0) = \sigma(\bar{D}^0) = \sigma(D^+) = \sigma(D^-)$ , and all contribute equally to neutrinos as observed in this and the BEBC experiment, the limits correspond to an upper limit for D-pair production of about  $100 \mu\text{b}$ , comfortably compatible with most of the values of Table IV (except the 15 mr BEBC result).

As can be seen in Table IV, our limits vary enormously depending on the model. If Lauterbach's polarization argument is correct, the CERN observations are probably not due to D production, but are some new phenomenon. Our upper limits are usually within a factor of two of the CERN 0 mr observations, sometimes higher and sometimes lower, depending on the model.

## VI AXIONS

The results of this experiment may also be interpreted to set limits on axion lifetimes and hence mass. The observed number of axions also follows from a relationship such as Eq. 1, although axion production may be expected to go as  $\sigma_I(NW)$ , so that  $F(NW)$  of Eq. 1 would be replaced by 1.12, not 4. There is also a factor for the decay of the axion,  $\exp(-7.3 \times 10^{-8}/\gamma\tau)$  over our 22 m target-detector separation. If  $E(\text{axion}) = 40$  GeV, the exponent is unity for  $\tau/m = 1.8 \times 10^{-12}$  (for  $m$  in MeV). The observed number of axion interactions  $N_A$  is then given by

$$N_A = N_P \left\{ \frac{\sigma_{PA}^{(W)} \times C}{\sigma_I(NW)} \right\} \left\{ \rho \ell \sigma_{IA} \right\} \left\{ \Delta\Omega_A(\text{M.C.}) \right\}, \quad (2)$$

where  $\sigma_{PA}^{(W)}$  and  $\sigma_{IA}$  are axion production (per tungsten nucleus) and interaction (per nucleon) cross sections respectively, and  $C$  is a correction factor for intra-target cascading, taken as unity. If  $\sigma_{PA}$  depends on  $A$  in the same way as the total inelastic cross section, the ratio  $\sigma_{PA}^{(W)}/\sigma_I(NW)$  may be reinterpreted as  $\sigma_{PA}^{(N)}/\sigma_I(NN)$ . The acceptance solid angle,  $\Delta\Omega_A(\text{M.C.})$  was determined (from a Monte Carlo calculation using  $d\sigma/dydp^2 = e^{-6m_\perp}$ , with  $m = 0.1 m_\pi$  and a uniform distribution in  $y$  over  $-2.5 < y < 2.5$ ). From this,  $\Delta\Omega_A(\text{M.C.}) = 0.09$ . The resulting number of "detected axions" is then:

$$N_A \approx 5 \times 10^{65} \sigma_{PA} \sigma_{IA}$$

If our 10 events are all axions, our results would yield

$$\sigma_{PA} \sigma_{IA} \approx 2 \times 10^{-65} \text{ cm}^4.$$

This may be compared with the prediction by Ellis and Gaillard<sup>11</sup> of

$$\sigma_{PA} \sigma_{IA} \geq 9 \times 10^{-66} \text{ cm}^4,$$

so that our results do not rule out axions. On the other hand, if most of our events are neutrinos, or if the theory limit is low, a lack of a positive axion signal in our data would suggest an axion mass greater than  $\sim 25$  MeV, as the stated axion lifetime is given<sup>12</sup> as

$$\tau = 10^{-10} \text{ sec}^2_{\alpha} \quad \text{or} \quad 10^{-10} \text{ csc}^2_{\alpha} \text{ (sec)}.$$

The factor C in Eq. (2) may in fact be somewhat greater than unity. If secondary protons and pions produce axions with cross sections in proportion to pion production, the overall thick target enhancement factor C may be 2-4. This would correspondingly reduce the product  $\sigma_{PA} \sigma_{IA}$  to below  $10^{-65} \text{ cm}^4$ , and thus significantly constrain possible axion production.

CONCLUSION

A positive signal for direct neutrino production is observed, although the background is  $\sim 1/3 - 1/2$  of the signal, and the statistical and systematic uncertainties are considerable. The data are consistent with the CERN BEBC results assuming  $A^1$  production dependence and a transverse momentum distribution as expected for a source of neutrinos from D-meson decays. The cross sections deduced are consistent with upper limits set by an earlier negative counter experiment. If the CERN beam-dump neutrinos were from  $\pi$  or K decay the lateral distribution would be narrow and the total number would be much less than we observed in our larger angular aperture detector.

## REFERENCES

1. W.P. Oliver, et al., TUFTS PUB 78-1601, to be published in the proceedings of the 3<sup>rd</sup> Int'l Conf. at Vanderbilt Univ. on New Results in H.E. Physics. (1978) and S. Childress et al., "A High Statistics Study of Dimuon Production by 400 GeV/c Protons" Sub. to XIX Int'l Conf. on H.E. Physics. Tokyo (1978) (unpublished).
2. L.W. Jones, et al., Nucl. Instr. and Methods 118, 431 (1974).
3. P. Alibrand, et al., Phys. Lett. 74B, 134 (1978);  
T. Hansl, et al., Phys. Lett. 74B, 143 (1978).  
P.C. Bosetti et al., Phys. Lett. 74B, 143 (1978).  
The data referenced in Table IV are from Bosetti et al.
4. L.W. Jones et al., UM HE 78-34, "The Muon Flux from E439 Beam Dump Targeting" (1978) (unpublished) and L.W. Jones UM HE 78-42 "Production Processes from Protons Incident on Thick Metal Targets (1978) (unpublished).
5. Review of Particle Properties LBL 100 and Phys. Lett. 75B, 1, (1978).
6. M.J. Lauterbach, Phys. Rev. D17, 2507 (1978).
7. H.D. Snyder et al., Phys. Rev. Lett. 36, 1415 (1976).
8. M. Binkley et al., Phys. Rev. Lett. 37, 574 (1976).
9. G.J. Blanaï, et al., Phys. Rev. Lett. 35, 346 (1976).
10. W.R. Ditzler, et al., Phys. Lett. 71B, 451 (1977).
11. J. Ellis and M.K. Gaillard, Phys. Lett. 74B, 374 (1978).
12. J. Ellis et al., Nucl. Phys. B106, 292 (1976).

Table I

Energies of prompt neutrino candidates from high intensity beam dump.

E (GeV)	20	21	24	26*	29	34*	46
	20*	21*	26	27	33	39*	98*

\*Accompanied by anomalous veto pulses (see text)

Table II

ns	Protons per pulse	Total targeted protons <sup>a</sup>	Pulses <sup>a</sup>	Mezzanine <sup>a</sup> counts	Muon telescope counts <sup>a</sup>	Events <sup>c</sup>
54,58	$1.4 \times 10^{11}$	$4.28 \times 10^{14}$	2929	$16 \times 10^6$	$19.3 \times 10^6$	8(14)
69,71	$1.3 \times 10^{10}$	$2.73 \times 10^{13}$	2091	$19.4 \times 10^6$	$29.3 \times 10^6$	6(9)
74-79	$2 \times 10^8$	$2.5 \times 10^{12}$	12,052	$14.5 \times 10^6$	—————	6(7)
104	—————	—————	239,000	—————	—————	74(103)

a. Corrected for dead time

b. Equivalent pulses

c. Total events without anticoincidence ADC cut in parentheses.

Table III Summary of events numbers with various selection and background criteria

RUN		54,58		69,71		74-79		69-79	
		(a)	(b)	(a)	(b)	(a)	(b)	(a)	(b)
a)	INCLUDE VETO ADC								
b)	IGNORE VETO ADC								
	Net events corrected for cosmic ray rate	7.1	12.8	5.4	8.2	2.3	2.3	7.7	10.5
	Beam dump events corrected assuming constant background per pulse, derived from runs as noted in column headings.	- .5	1.4	6.5	12.2	5.5	10.6		
	Beam dump events corrected assuming background correlated with mezzanine flux, derived from runs as noted in column headings.	2.8	6.1	4.7	10.2	3.4	7.9		
	Beam dump events, weighted 3/4 mezzanine background, 1/4 pulse background	2.0	5.3	5.2	10.7	3.9	8.6		
	Overall net beam dump events weighted by self-veto correction factor K = 1.6	3.2	8.5	8.3	17	6.2	13.8		

Table IV

Cross Sections for Production of D-Pairs<sup>1</sup>

Model <sup>2</sup>	$\gamma$ limit	This Experiment			CERN BEBC	
		Probability $G(E)\Delta\Omega$ (M.C.) for $E > 20$ GeV released in cal.	$\bar{E}_\nu$	$\sigma$ ( $\mu\text{b}$ ) <sup>4</sup>	$\sigma$ ( $\mu\text{b}$ ) <sup>5</sup>	$\sigma$ ( $\mu\text{b}$ ) <sup>6</sup>
Ia	0.5	0.008	26	700	500	900
Ib	1.5	0.052	51	60	50	200
Ic	2.5	0.131	87	17	5	150
IIa		.020	52	202	128	532
IIb		.05	54	76	46	285
IIIa		.102	55	37	25	115
IIIb		.115	54	33	22	122
IV		0.042	49	75	45	240

1. Semileptonic decays of D's of 20% assumed source of  $\nu$ ; equal numbers of  $\nu_e, \bar{\nu}_e, \nu_\mu, \bar{\nu}_\mu$

2. See text for details of models

3. Based on Monte Carlo calculation of 30,000 events.  $G(E)\Delta\Omega$ (M.C.) defined in text.

4. Based on a signal of 10 events. See text for systematic errors.

5. Based on 15  $e^+, e^-$  events. (see Ref. 3)

6. Based on 8  $e^-$  events (Ref. 3).

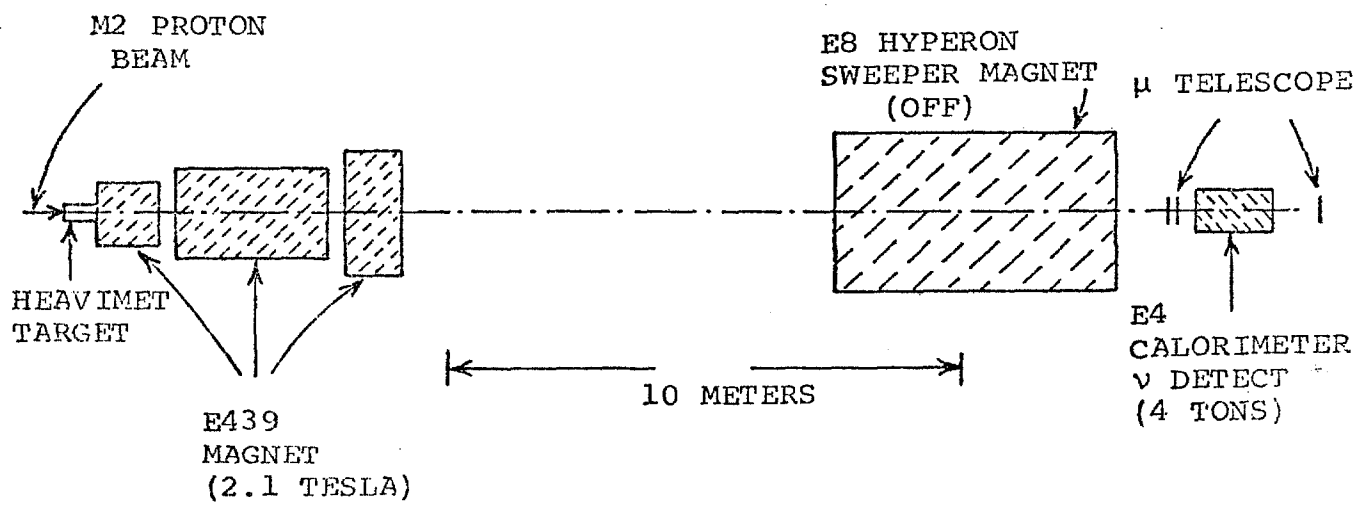
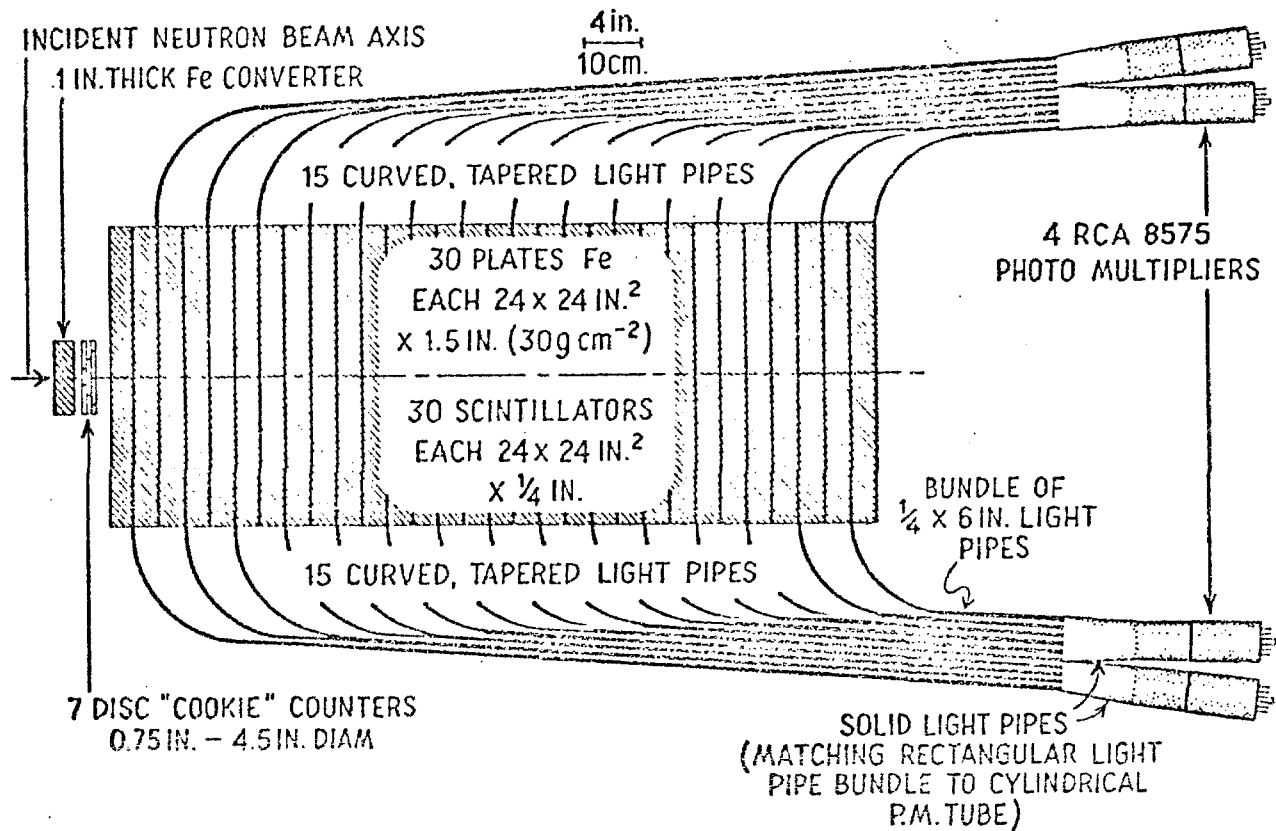


FIGURE 1  
 EXPERIMENT  
 CONFIGURATION



MICHIGAN NEUTRON CALORIMETER

FIGURE 2

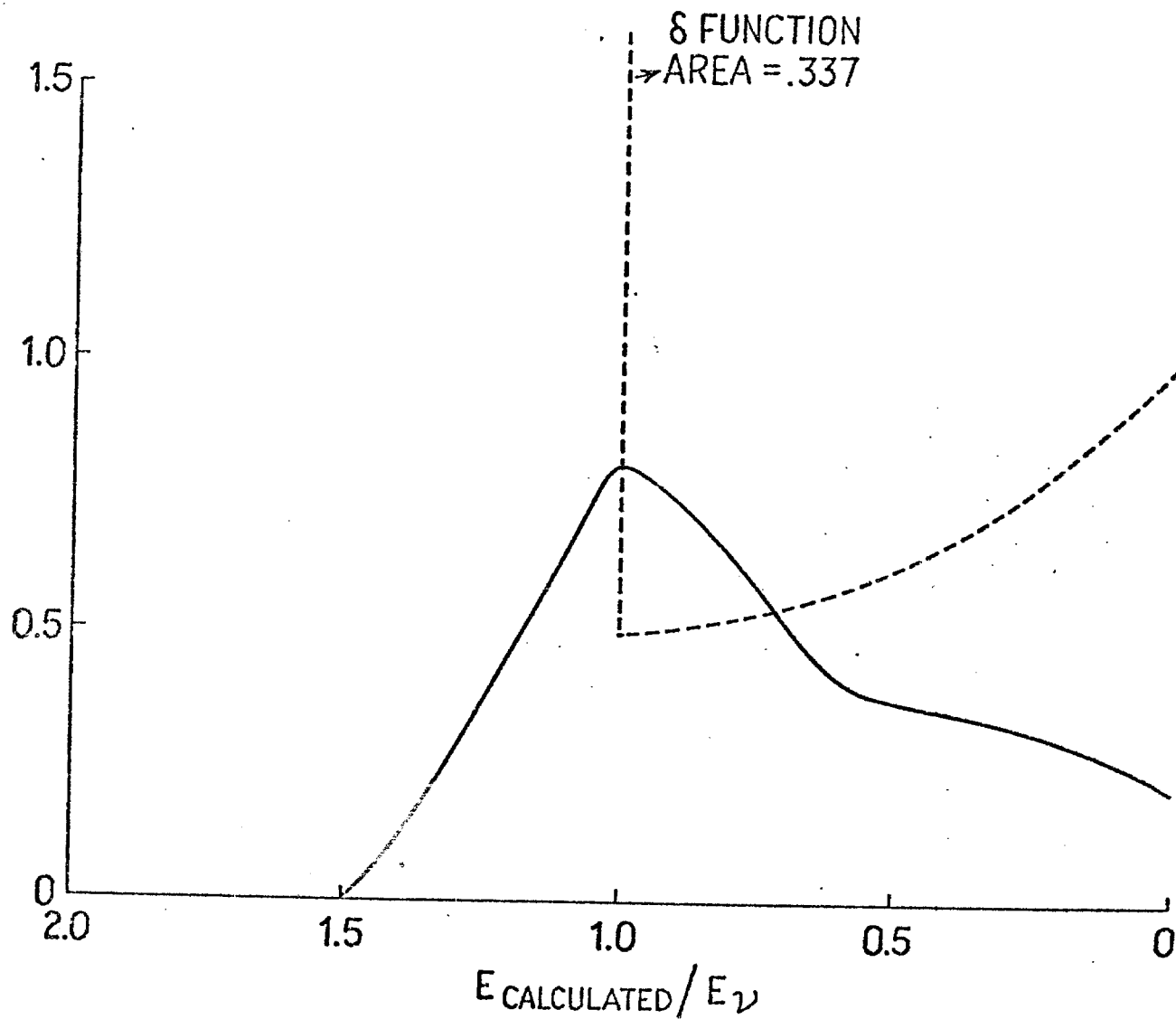


Figure 3: Energy deposited in calorimeter per incident neutrino, averaged over  $\nu_e, \bar{\nu}_e$  and  $\nu_{\mu}, \bar{\nu}_{\mu}$ . The dashed line is for "perfect" calorimeter response (pulse height exactly proportional to the sum of hadron and electron reaction products). The smooth curve is for a calorimeter with Gaussian resolution,  $\sigma = 0.21E$ .

APPENDIX B

Performance of the Lead Scintillator Shower Counters.

P. Copper, M. Gilckries, M. Heagy, R. Imlay,  
T.Y. Ling, A.K. Mann, M. Merlin, S. Mori,  
D.D. Reader, R. Stefanski, T. Trinko and D. Winn

University of Wisconsin  
University of Pennsylvania  
Rutgers University  
Ohio State University  
Fermi National Accelerator Laboratory

Appendix <sup>B</sup>A - Performance of the Lead-Scintillator Shower Counters.

We have tested one module of the lead-scintillator calorimeter in the M5 meson area beam. A drawing of one such shower counter is given in Fig. 1. Each module consists of five optically separate strips, 27 cm wide and 365 cm long, with 2" phototubes (RCA 6655 for these tests) mounted on each end. Within each strip there are 12  $\frac{1}{2}$ " thick teflon coated lead plates (total of 13.6 radiation lengths) with  $\frac{1}{4}$ " gaps between plates filled with liquid scintillator (NE235A). The lead sheets extend to within 30 cm of the edge of the counter. The remaining space is taken up by reflectors to collect and channel light to the phototubes.

Tests were performed to determine the response of the counter to minimum ionizing particles and electrons. Electrons in the M5 beam (~4% of the particles) were identified by a threshold Cerenkov counter. Two overlapping scintillation counters immediately upstream of the test module, in coincidence with beamline counters, defined the beam. LeCroy 2249A ADC's were used to record anode and inverted dynode signals from the photomultipliers. Data were recorded on magnetic tape and extensively analyzed on-line using a modified version of the E-310 data acquisition program resident in the Detector Development PDP 11/20 computer.

1) Response to Minimum Ionizing Particles

In order to test the response to minimum ionizing particles, one strip of the module was centered, vertically and horizontally, on the beam center line. The right (R) and left (L) phototube voltages were then adjusted to yield equal response from each tube. A typical distribution of the sum of the right and left pulse heights is shown in Fig. 2. Minimum ionizing particles are clearly visible with good efficiency.

The uniformity of response along the horizontal direction was also determined. The sum of the right and left tubes at the center of the counter is shown in Fig. 3 for various horizontal positions. The total pulse height increases by 80% at 120 cm and grows rapidly thereafter as the edge of the lead sheets (150 cm) is approached. Since a reasonable fiducial cut would be  $\sim 120$  cm, the observed response will be sufficiently uniform.

The response to movement of the beam in the vertical direction is shown in Fig. 4 for two different horizontal positions - center of the counter ( $X = 0$ ) and  $x = 120$  cm. The light output shows no variation with vertical position.

We have also determined the horizontal attenuation length in the counter. In Fig. 5 we plot the ratio of the right to left pulse heights (R/L) as a function of horizontal position. The observed ratios clearly suggest an exponential fall-off in light intensity for each tube with an attenuation length of 1.1 m.

#### ii) Response to Electrons

We have measured the response of the test module to 10, 20, 30 and 39.3 Gev electrons. The distribution for 30 Gev electrons is shown in Fig. 6a. In Fig. 7 we plot the measured electron energy vs the beam momentum assuming that the electron shower is totally contained in the counter at 10 Gev. A deviation from linear dependence is evident at 30 and 39.3 Gev, indicative of energy leakage from the counter.

The positional dependence of the light output for electrons is the same in the horizontal direction as for minimum ionizing particles and

differ in the vertical direction only in the vicinity of the spacer bar between strips. This inactive region causes an apparent loss of energy as shown in Fig. 8 where we plot the energy response vs vertical position.

The shower energy resolution at 10, 20, 30 and 39.3 Gev was also determined. The full-width-at-half maximum (FWHM) at each energy was determined by doubling the half-width on the higher energy side of the shower peak. This was made necessary by a considerable radiative tail as a result of material in the M5 beam as may be seen in the logarithmic plot of Fig. 6b. Furthermore, the intrinsic momentum spread for electrons in the M5 is known to be larger than the calculated  $\pm 1\%$ . We therefore believe our measurements to be upper bounds on the electromagnetic energy resolution of a single calorimeter module.

The measured resolutions (FWHM) are plotted in Fig. 9. They vary from 23% at 10 Gev to 10% at 30 and 39.3 Gev.

### iii) Summary

The tests described above have demonstrated that the lead-scintillation calorimeters respond with good efficiency to minimum ionizing particles with reasonable uniformity over the useful area of the counter. These counters should also be able to identify and measure electromagnetic showers with adequate resolution.

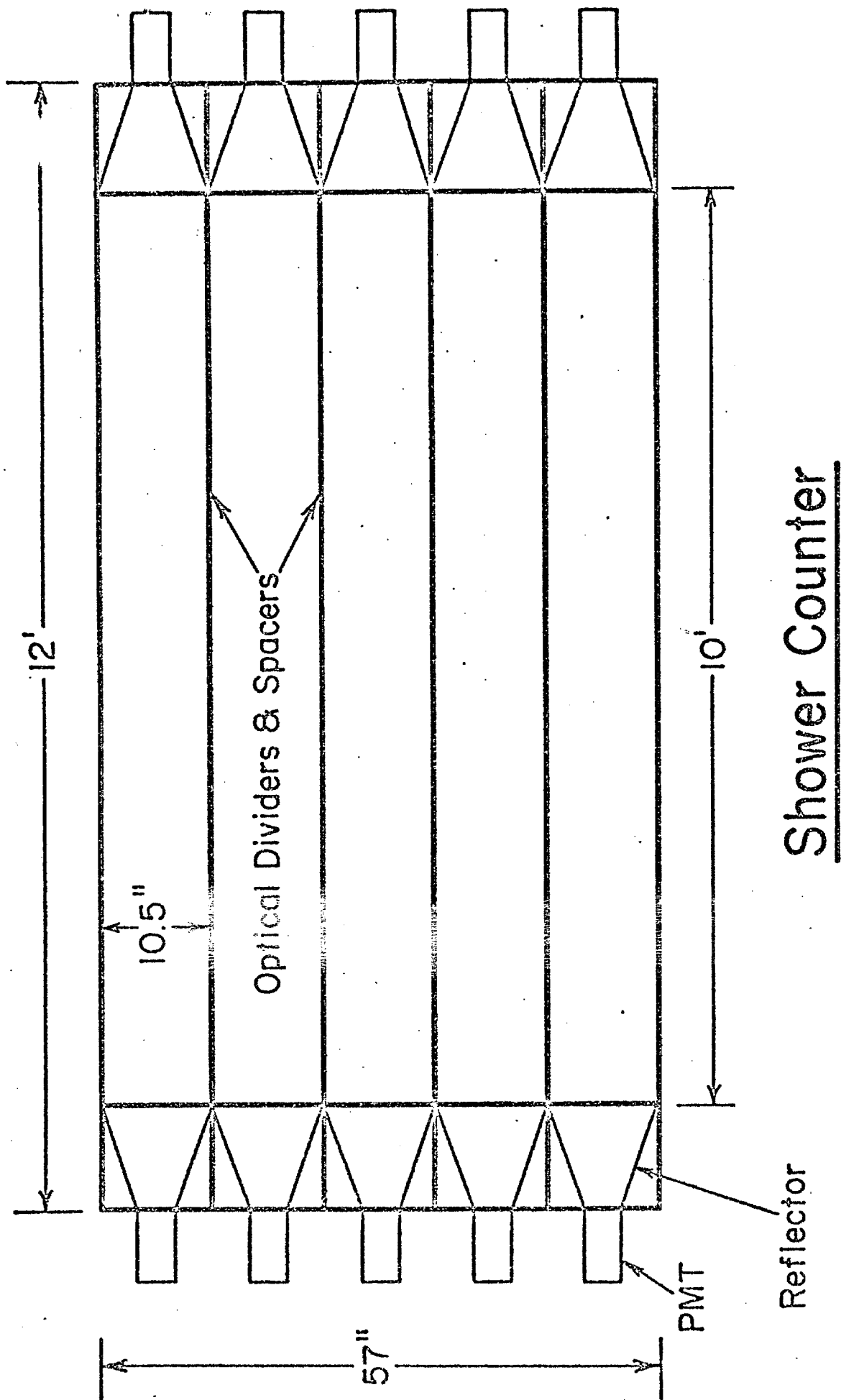


Fig. 1

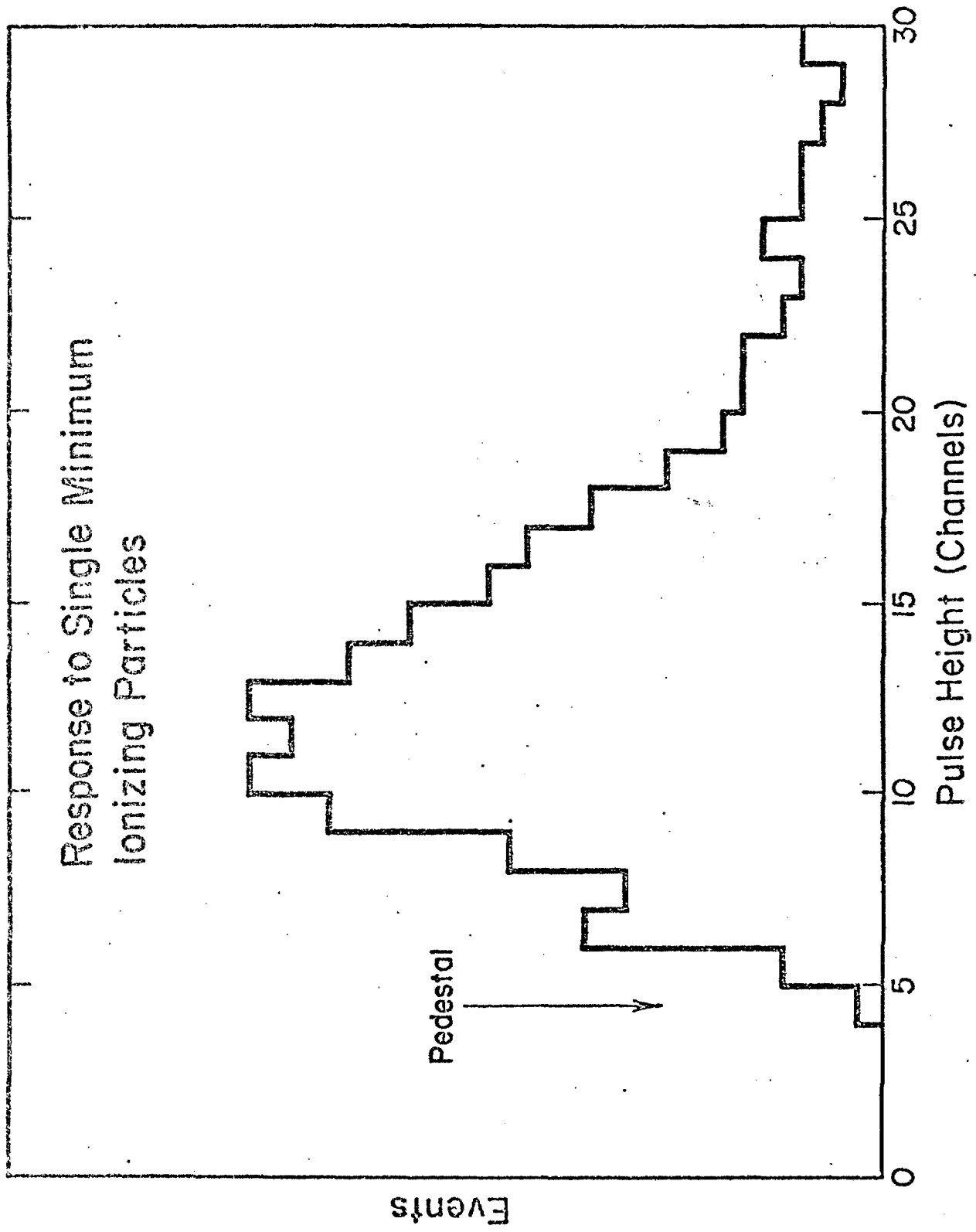


Fig. 2

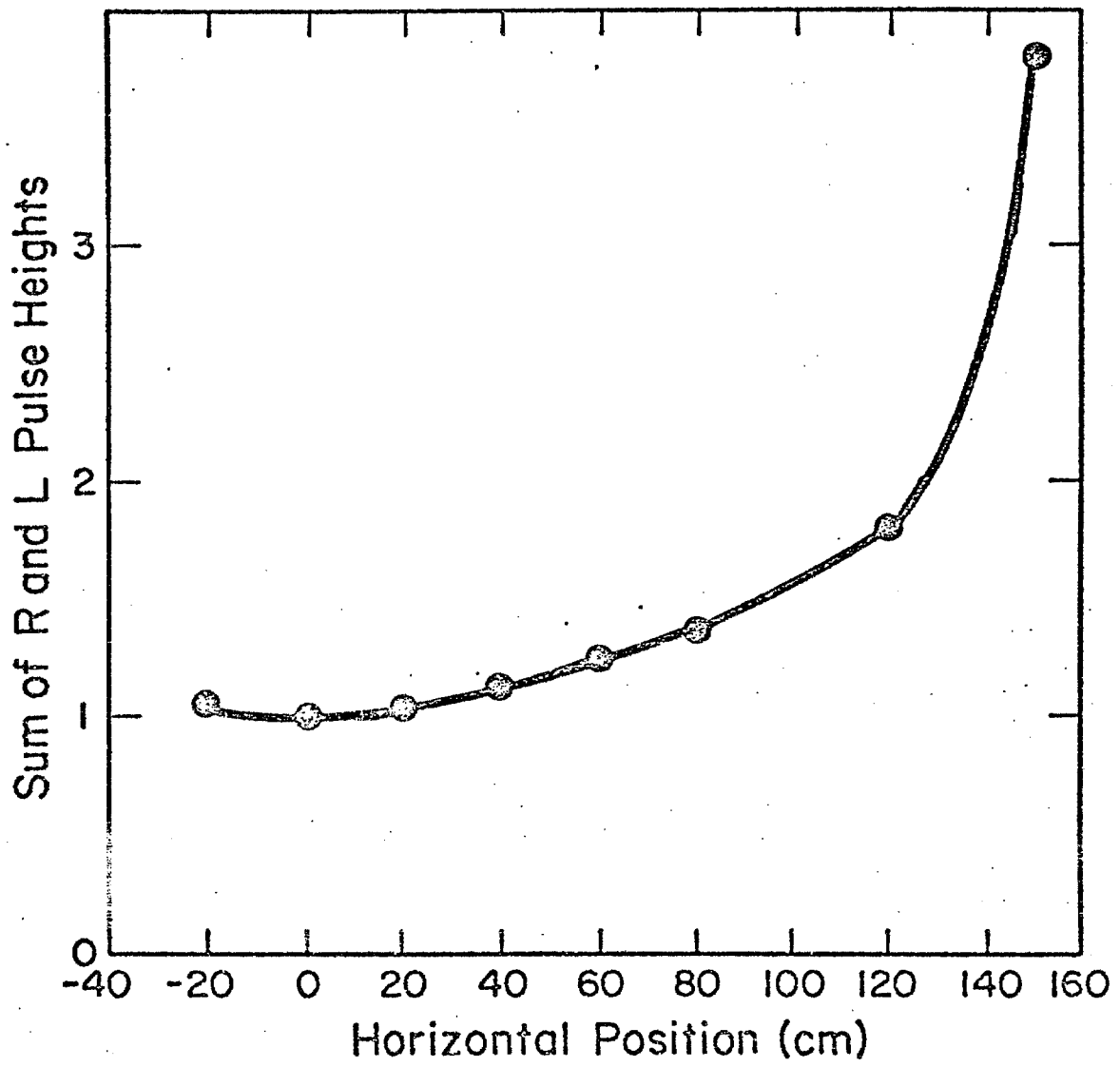


Fig. 3

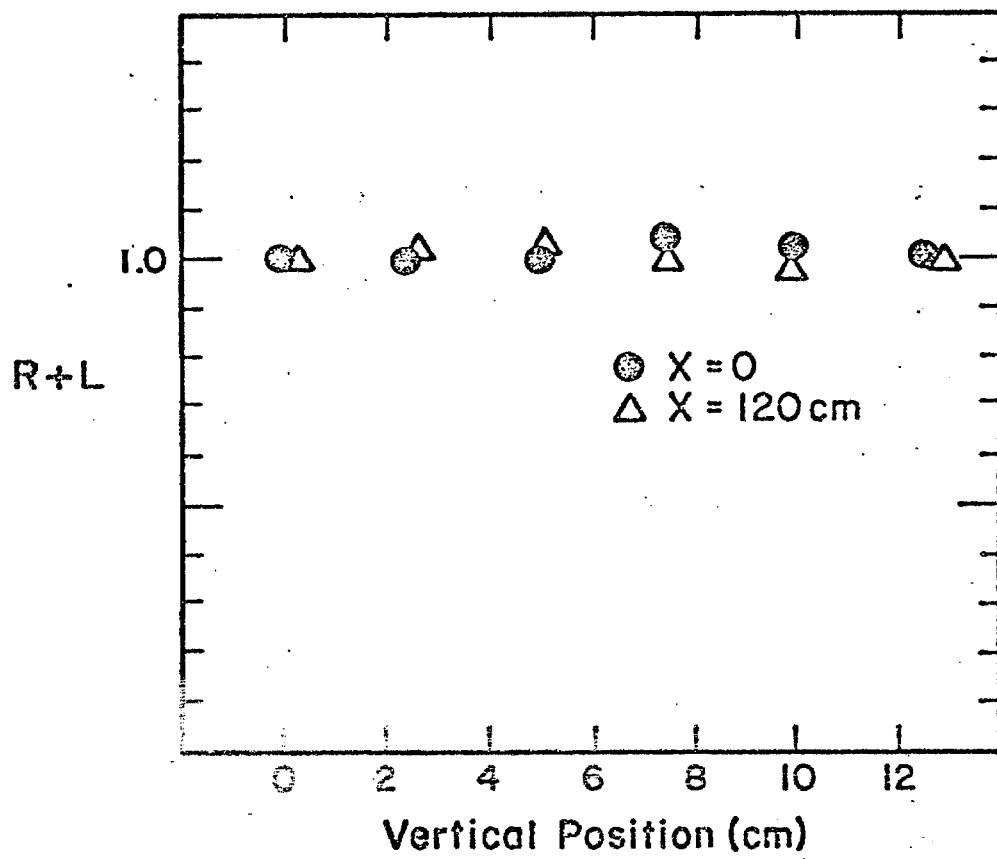


Fig. 4

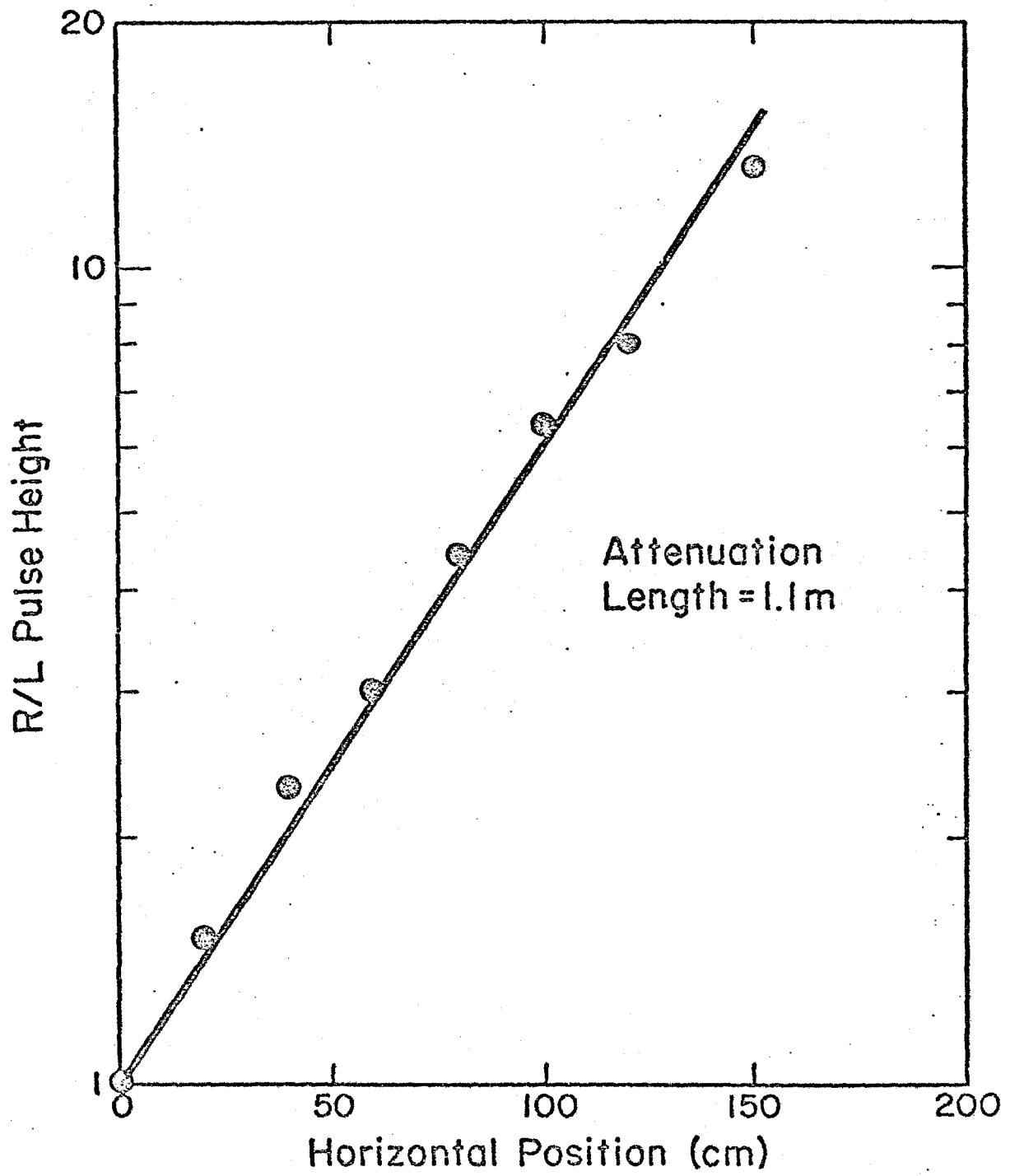
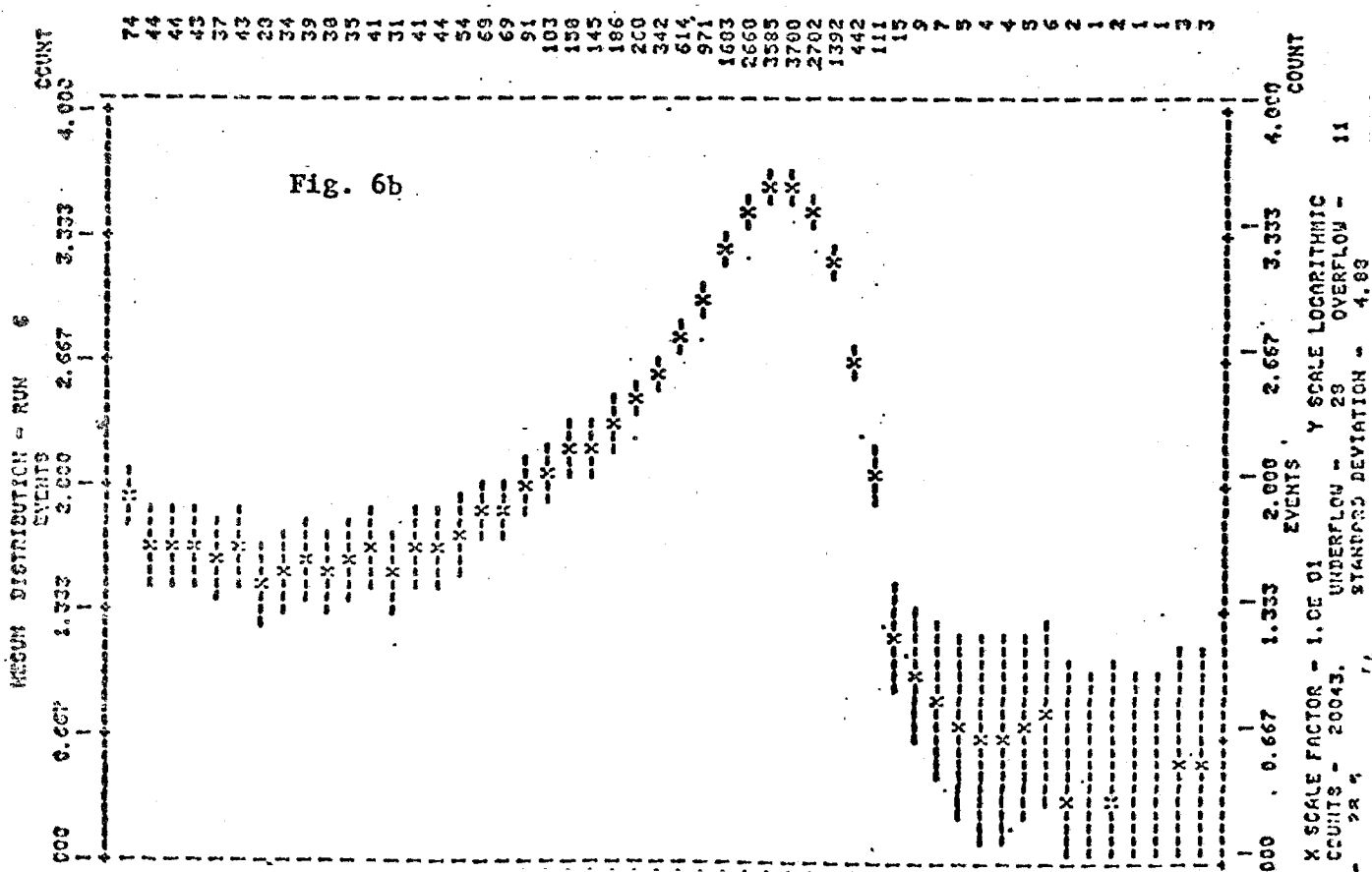
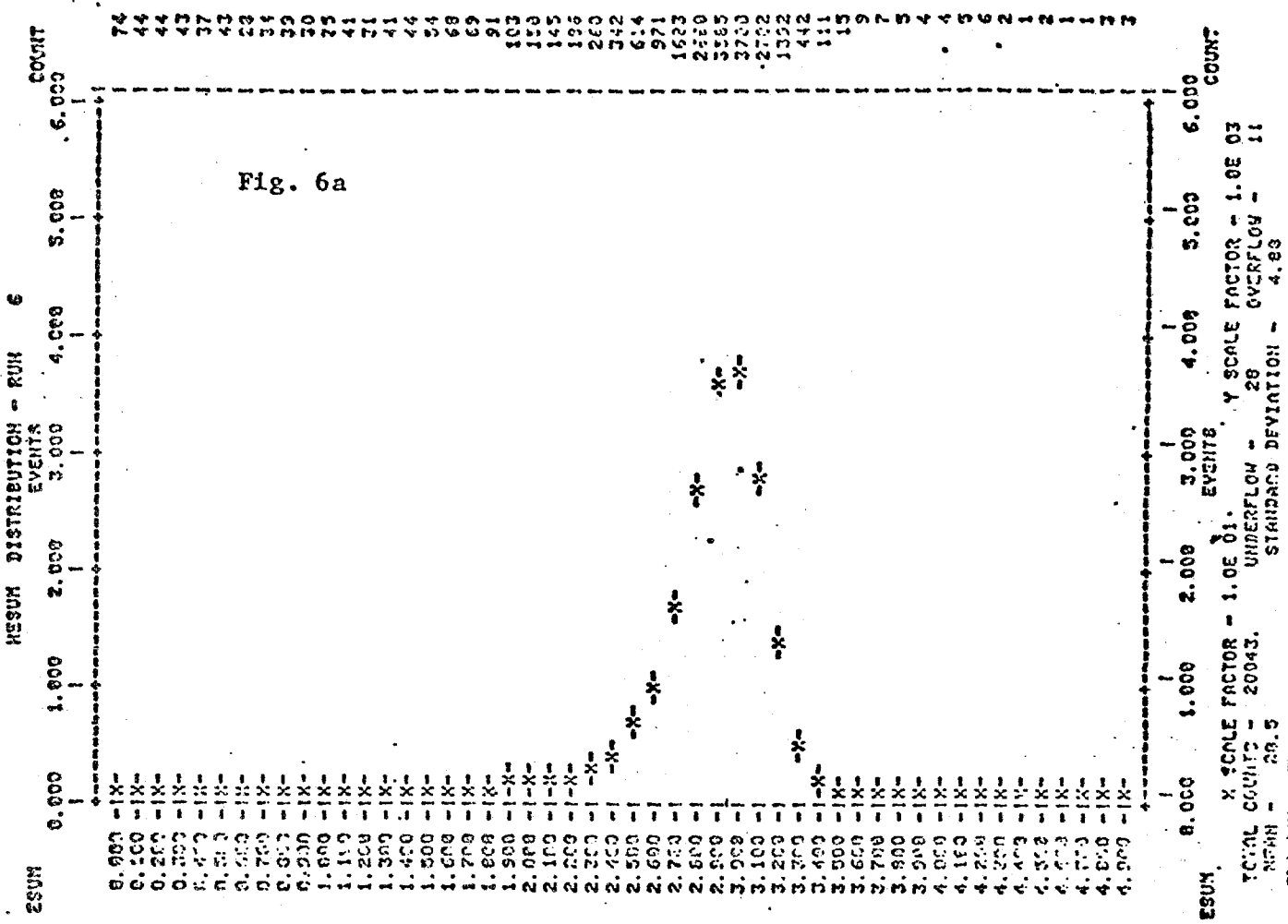


Fig. 5

Figure 6



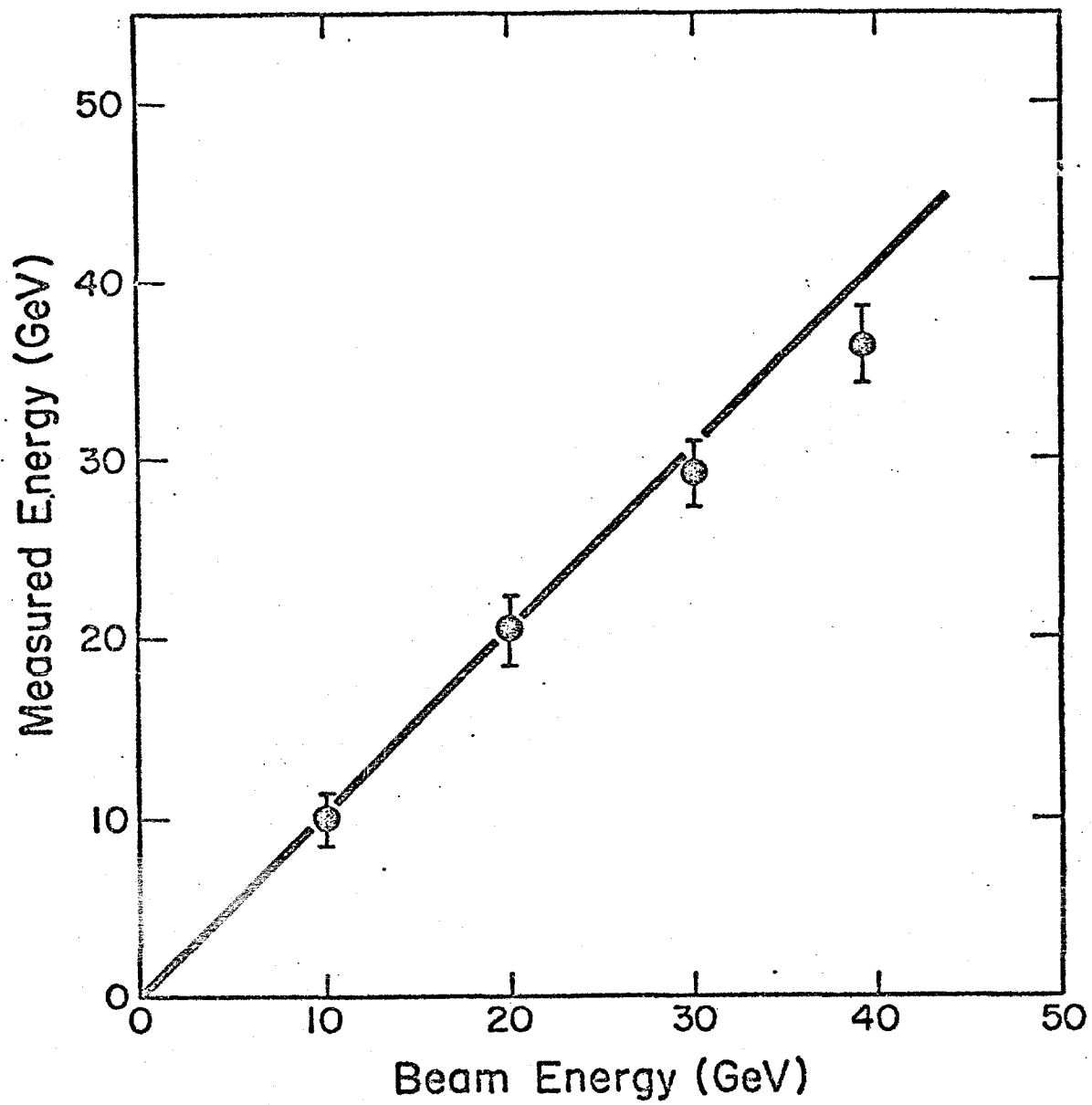


Fig. 7

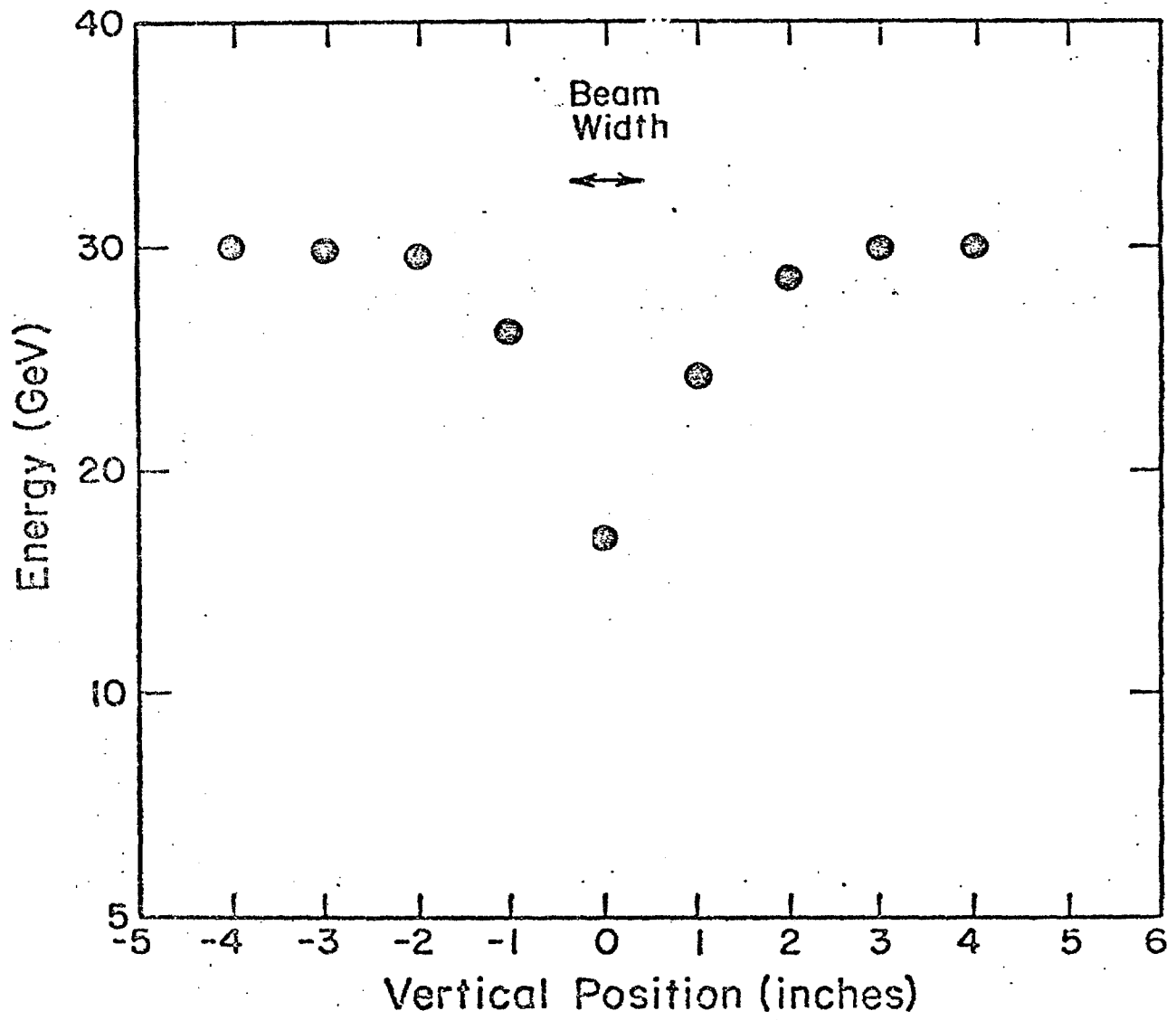


Fig. 8

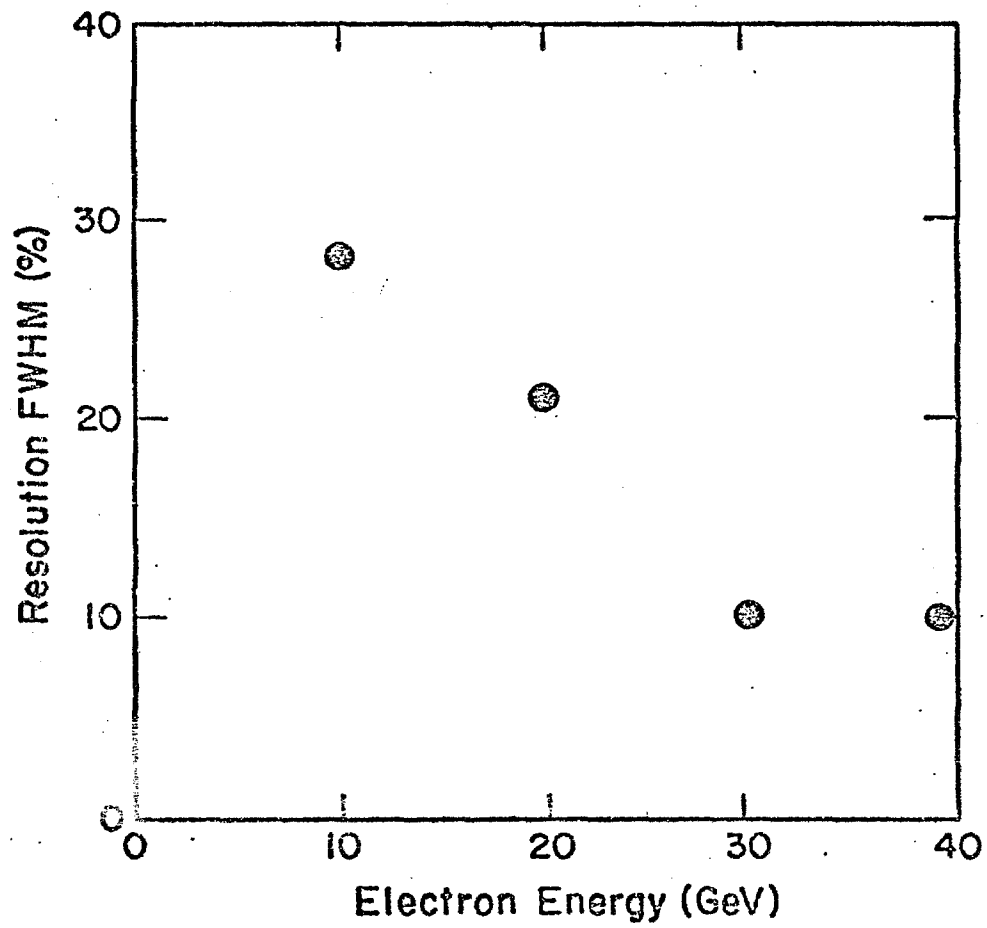


Fig. 9

APPENDIX B

Performance of the Lead Scintillator Shower Counters.

P. Copper, M. Gilckries, M. Heaggy, R. Imlay,  
T.Y. Ling, A.K. Mann, M. Merlin, S. Mori,  
D.D. Reader, R. Stefanski, T. Trinko and D. Winn

University of Wisconsin  
University of Pennsylvania  
Rutgers University  
Ohio State University  
Fermi National Accelerator Laboratory

Appendix <sup>B</sup>A - Performance of the Lead-Scintillator Shower Counters.

We have tested one module of the lead-scintillator calorimeter in the M5 meson area beam. A drawing of one such shower counter is given in Fig. 1. Each module consists of five optically separate strips, 27 cm wide and 365 cm long, with 2" phototubes (RCA 6655 for these tests) mounted on each end. Within each strip there are 12  $\frac{1}{4}$ " thick teflon coated lead plates (total of 13.6 radiation lengths) with  $\frac{1}{4}$ " gaps between plates filled with liquid scintillator (NE235A). The lead sheets extend to within 30 cm of the edge of the counter. The remaining space is taken up by reflectors to collect and channel light to the phototubes.

Tests were performed to determine the response of the counter to minimum ionizing particles and electrons. Electrons in the M5 beam (~4% of the particles) were identified by a threshold Cerenkov counter. Two overlapping scintillation counters immediately upstream of the test module, in coincidence with beamline counters, defined the beam. LeCroy 2249A ADC's were used to record anode and inverted dynode signals from the photomultipliers. Data were recorded on magnetic tape and extensively analyzed on-line using a modified version of the E-310 data acquisition program resident in the Detector Development PDP 11/20 computer.

1) Response to Minimum Ionizing Particles

In order to test the response to minimum ionizing particles, one strip of the module was centered, vertically and horizontally, on the beam center line. The right (R) and left (L) phototube voltages were then adjusted to yield equal response from each tube. A typical distribution of the sum of the right and left pulse heights is shown in Fig. 2. Minimum ionizing particles are clearly visible with good efficiency.

The uniformity of response along the horizontal direction was also determined. The sum of the right and left tubes at the center of the counter is shown in Fig. 3 for various horizontal positions. The total pulse height increases by 80% at 120 cm and grows rapidly thereafter as the edge of the lead sheets (150 cm) is approached. Since a reasonable fiducial cut would be  $\sim 120$  cm, the observed response will be sufficiently uniform.

The response to movement of the beam in the vertical direction is shown in Fig. 4 for two different horizontal positions - center of the counter ( $X = 0$ ) and  $x = 120$  cm. The light output shows no variation with vertical position.

We have also determined the horizontal attenuation length in the counter. In Fig. 5 we plot the ratio of the right to left pulse heights ( $R/L$ ) as a function of horizontal position. The observed ratios clearly suggest an exponential fall-off in light intensity for each tube with an attenuation length of 1.1 m.

#### ii) Response to Electrons

We have measured the response of the test module to 10, 20, 30 and 39.3 Gev electrons. The distribution for 30 Gev electrons is shown in Fig. 6a. In Fig. 7 we plot the measured electron energy vs the beam momentum assuming that the electron shower is totally contained in the counter at 10 Gev. A deviation from linear dependence is evident at 30 and 39.3 Gev, indicative of energy leakage from the counter.

The positional dependence of the light output for electrons is the same in the horizontal direction as for minimum ionizing particles and

differ in the vertical direction only in the vicinity of the spacer bar between strips. This inactive region causes an apparent loss of energy as shown in Fig. 8 where we plot the energy response vs vertical position.

The shower energy resolution at 10, 20, 30 and 39.3 Gev was also determined. The full-width-at-half maximum (FWHM) at each energy was determined by doubling the half-width on the higher energy side of the shower peak. This was made necessary by a considerable radiative tail as a result of material in the M5 beam as may be seen in the logarithmic plot of Fig. 6b. Furthermore, the intrinsic momentum spread for electrons in the M5 is known to be larger than the calculated  $\pm 1\%$ . We therefore believe our measurements to be upper bounds on the electromagnetic energy resolution of a single calorimeter module.

The measured resolutions (FWHM) are plotted in Fig. 9. They vary from 23% at 10 Gev to 10% at 30 and 39.3 Gev.

### iii) Summary

The tests described above have demonstrated that the lead-scintillation calorimeters respond with good efficiency to minimum ionizing particles with reasonable uniformity over the useful area of the counter. These counters should also be able to identify and measure electromagnetic showers with adequate resolution.

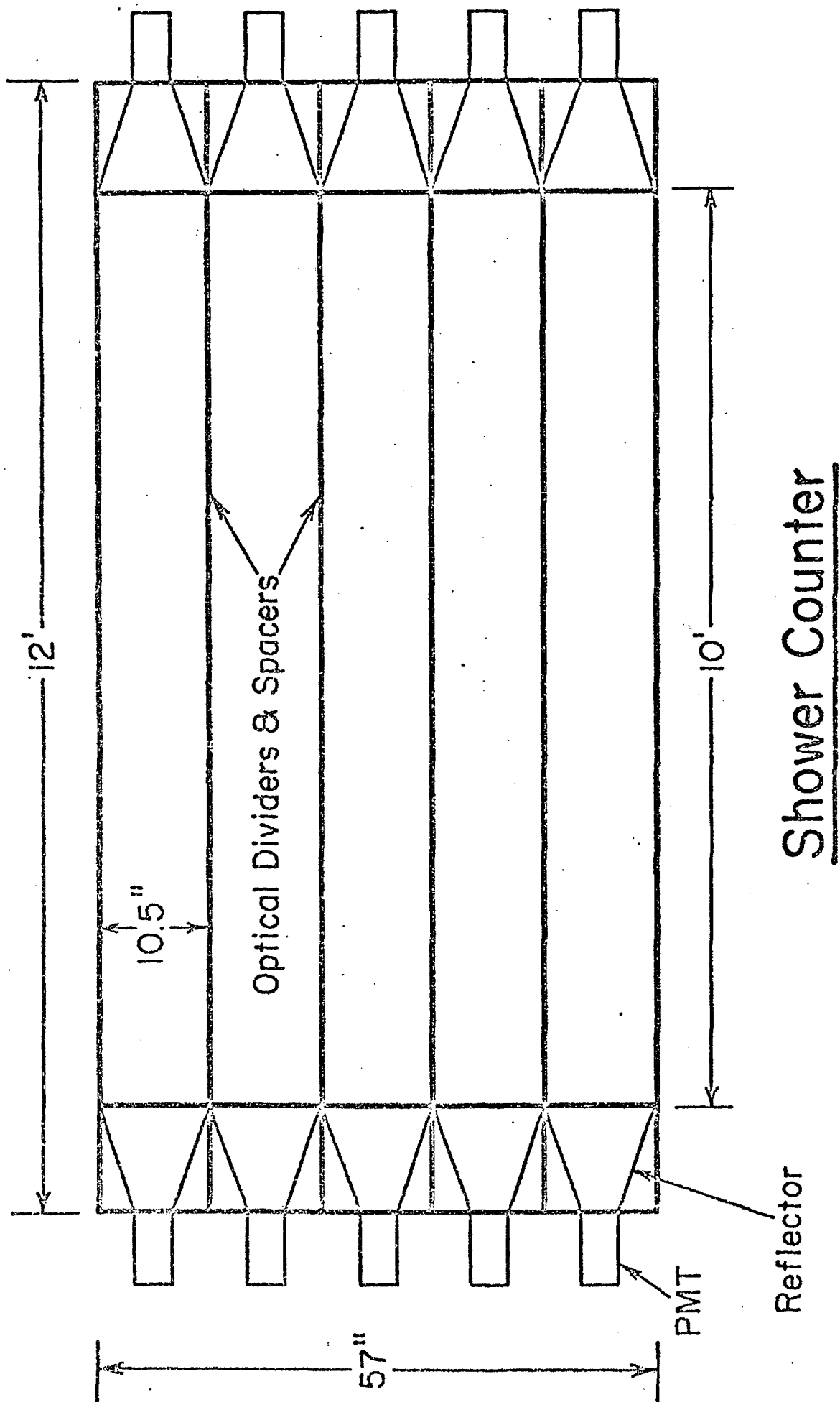


Fig. 1

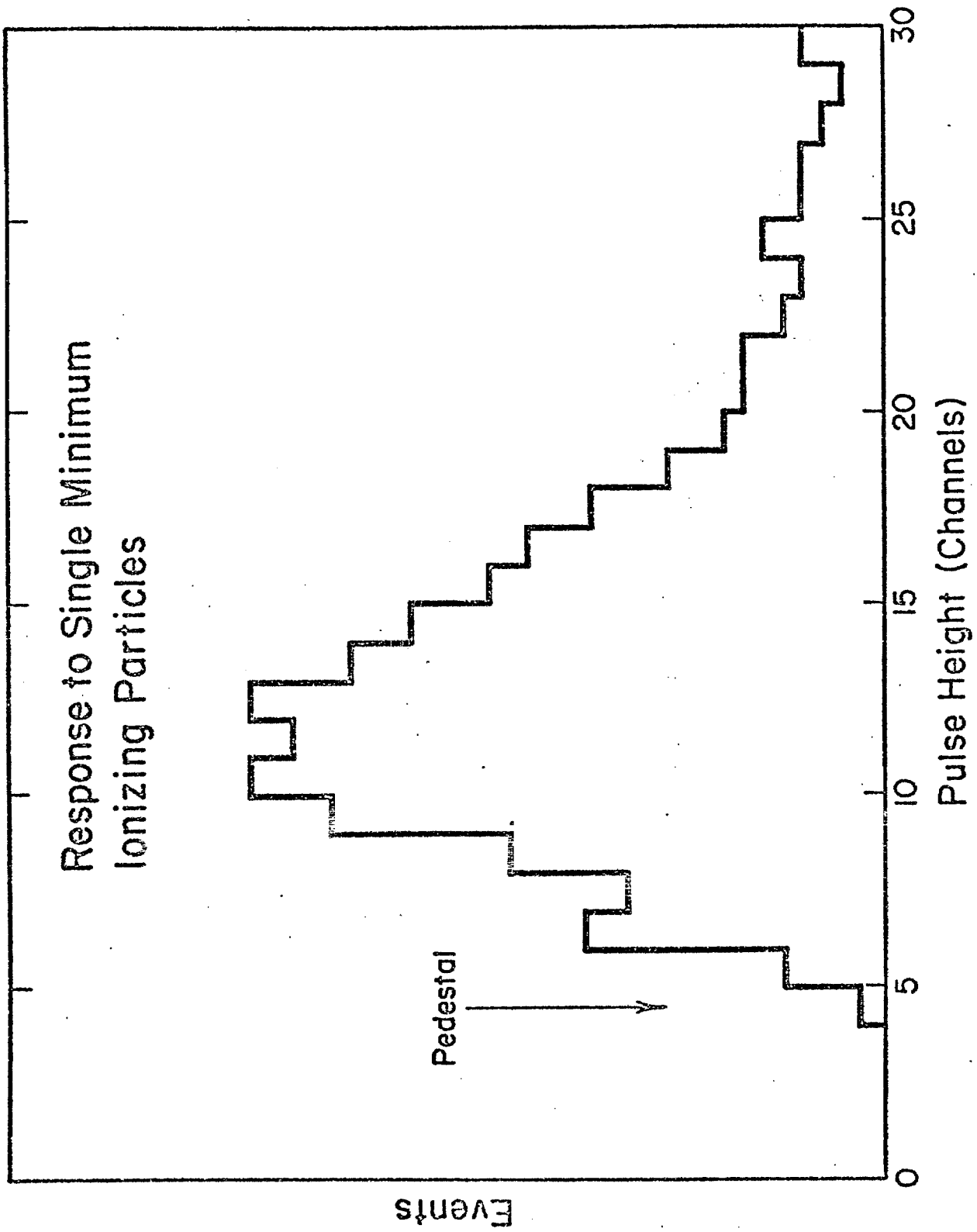


Fig. 2

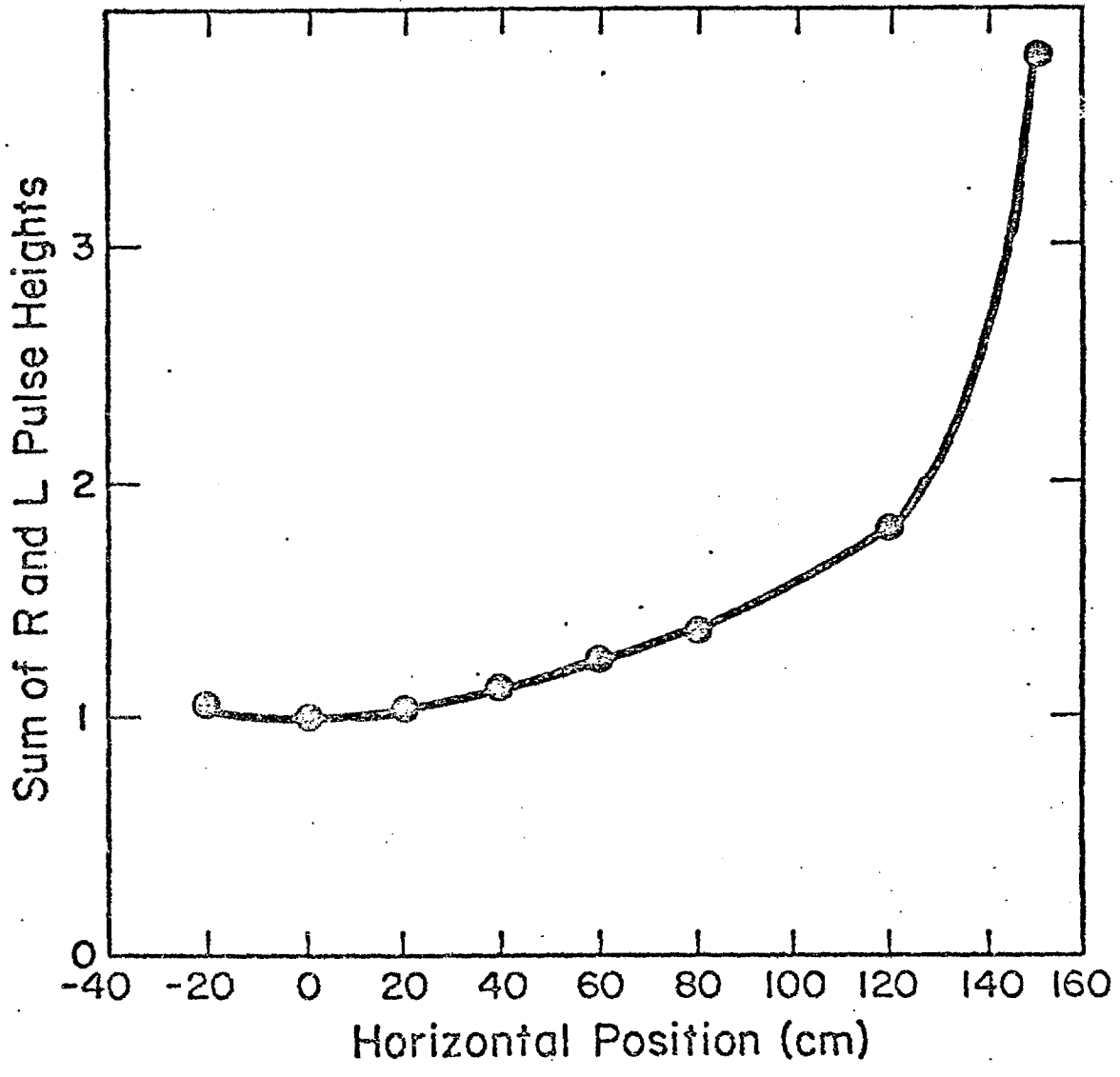


Fig. 3

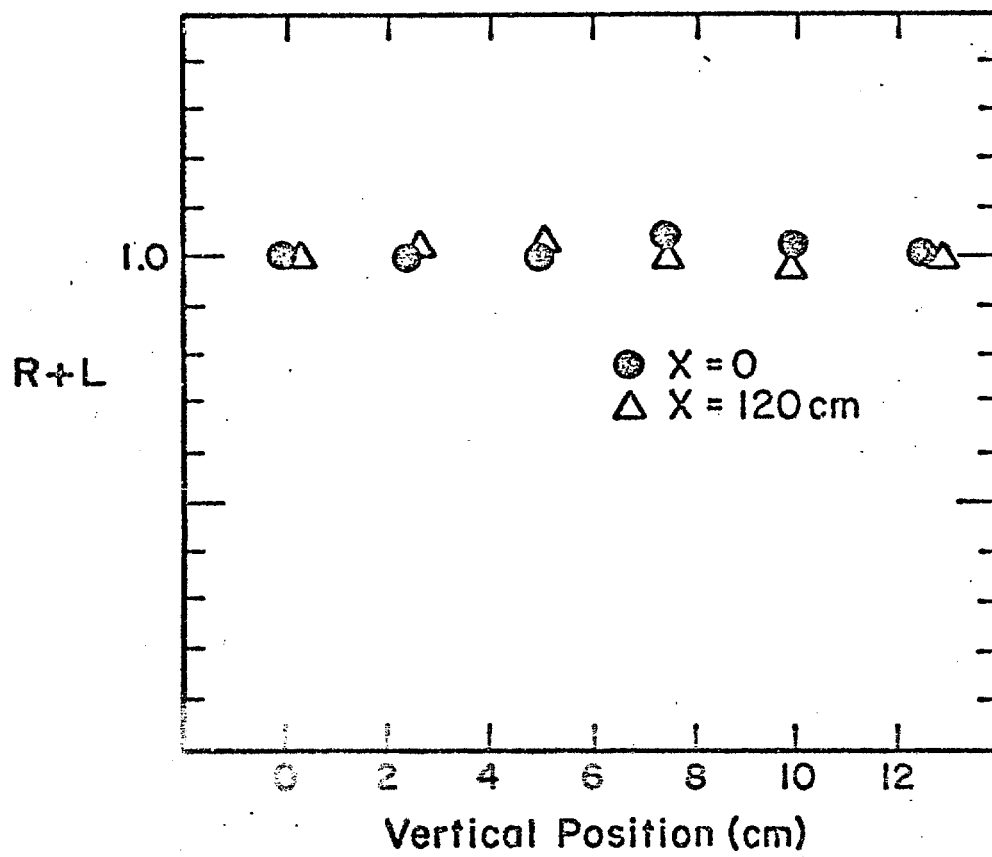


Fig. 4

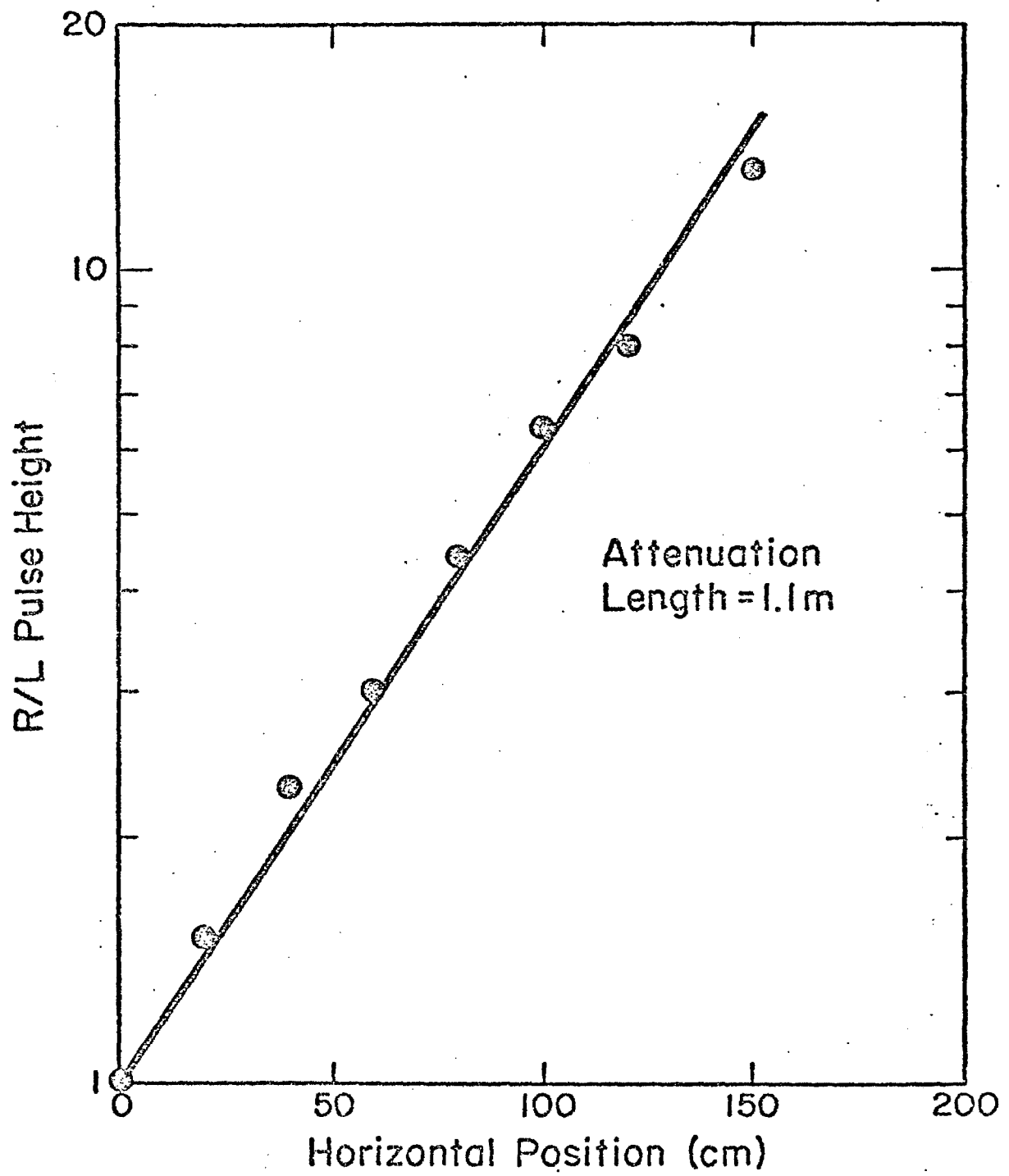
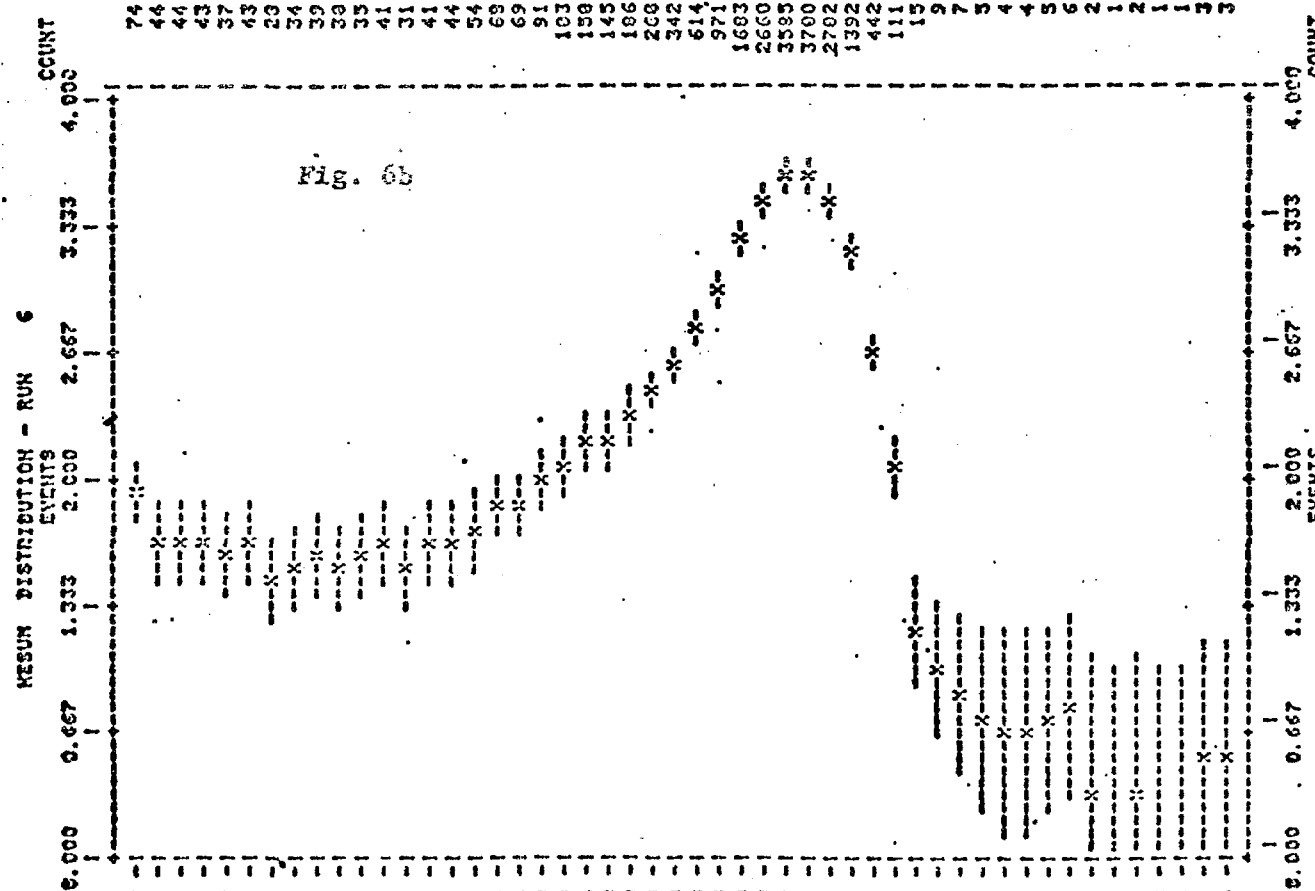
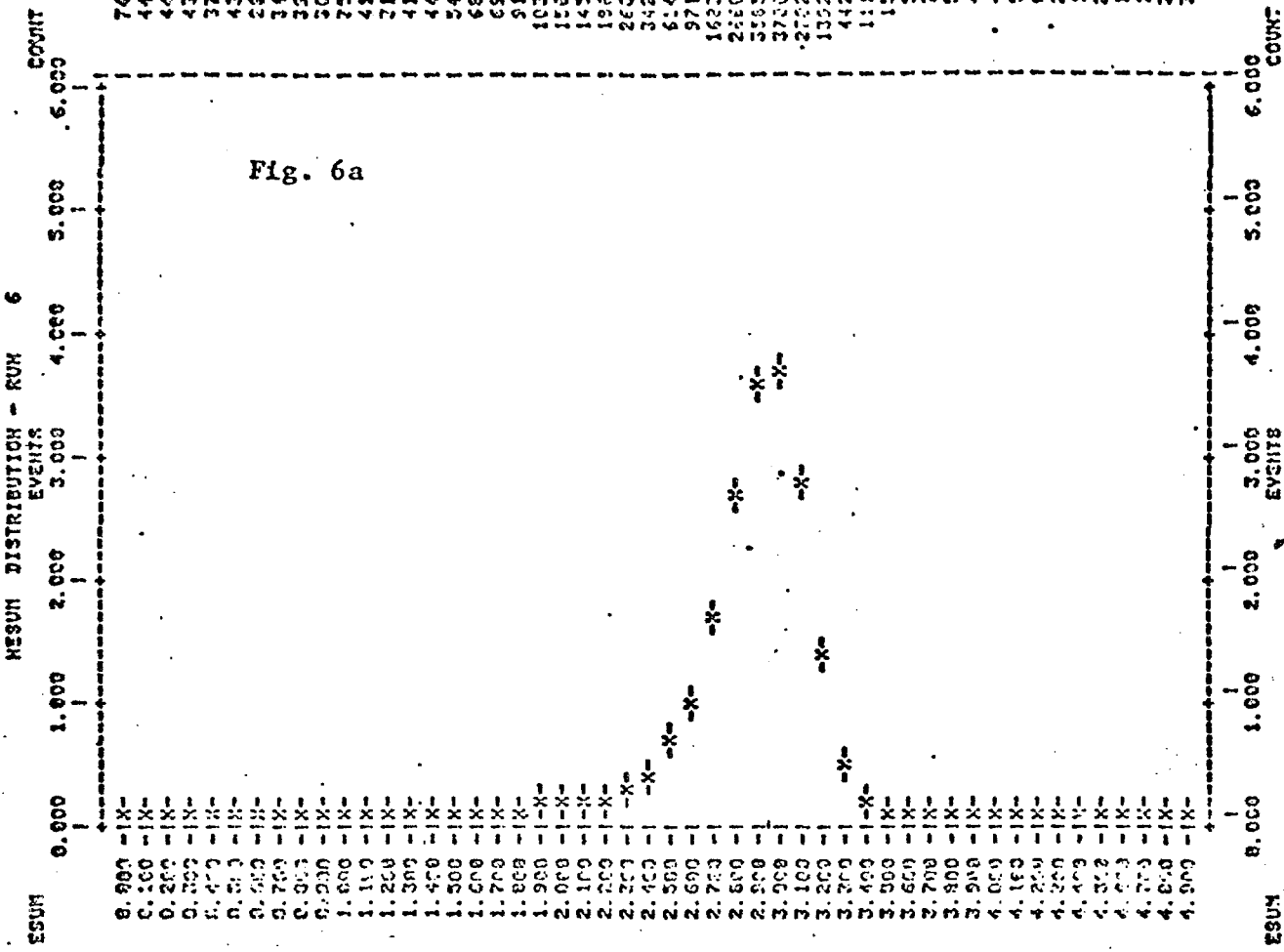


Fig. 5

Figure 6



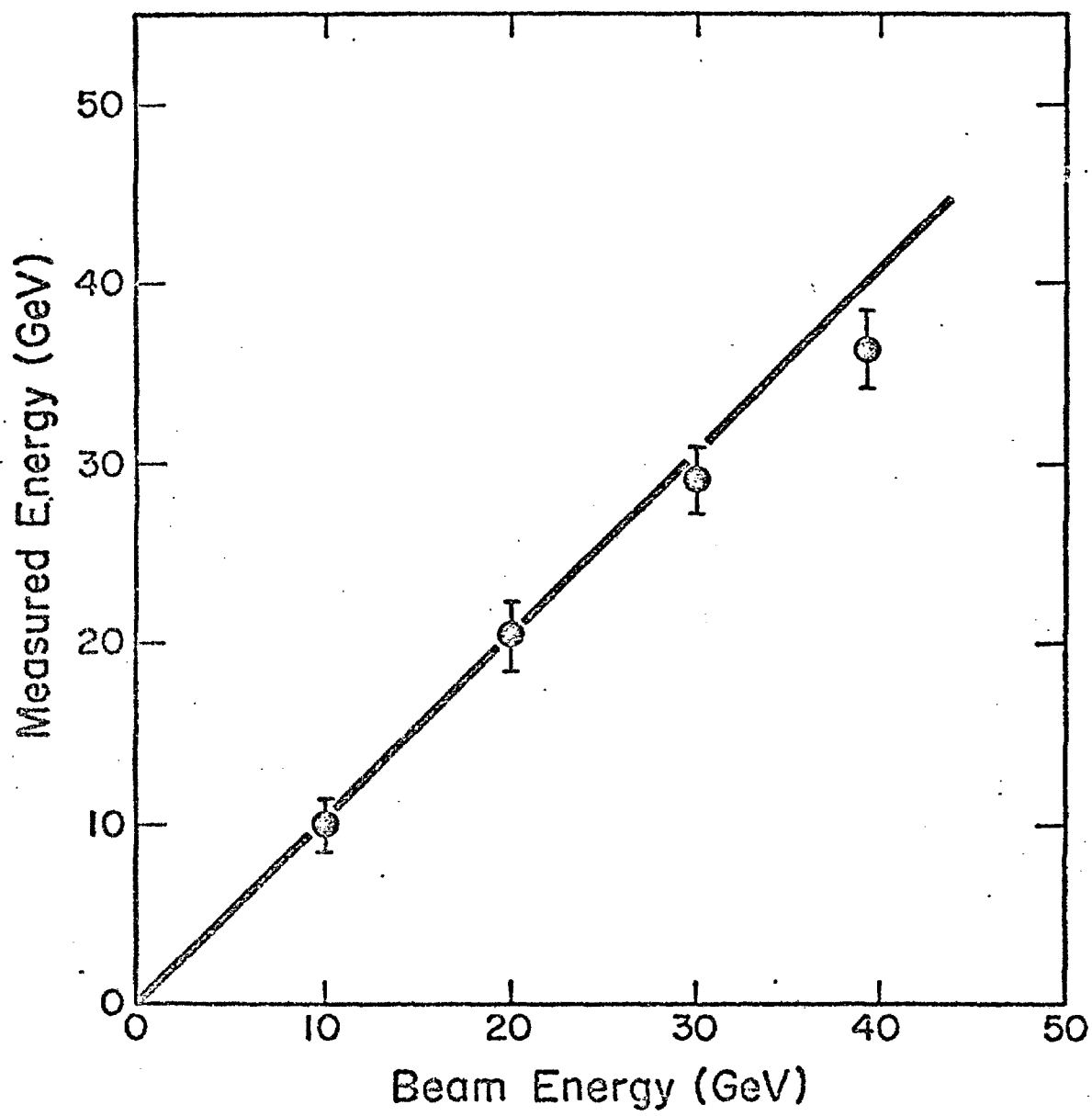


Fig. 7

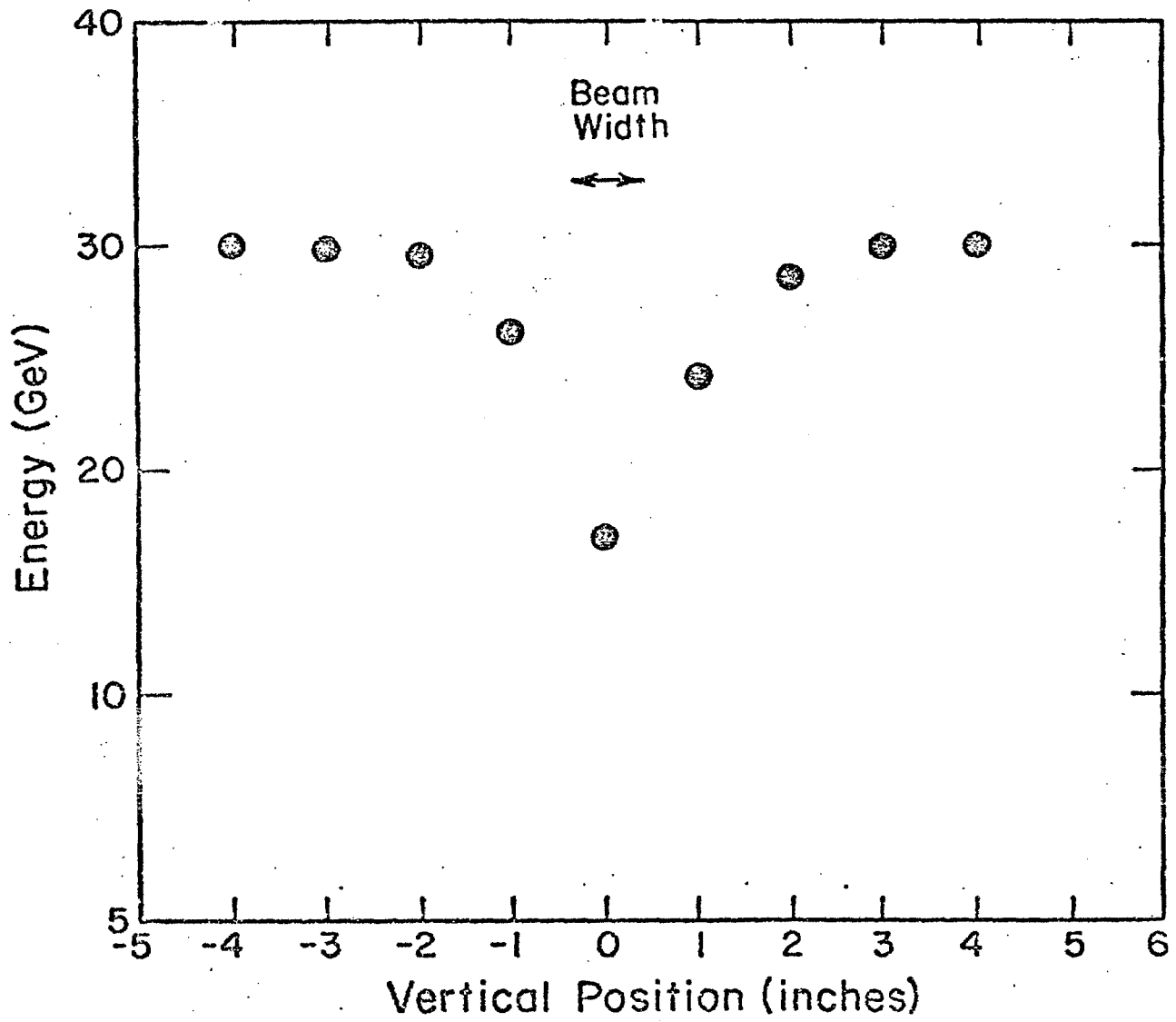


Fig. 8

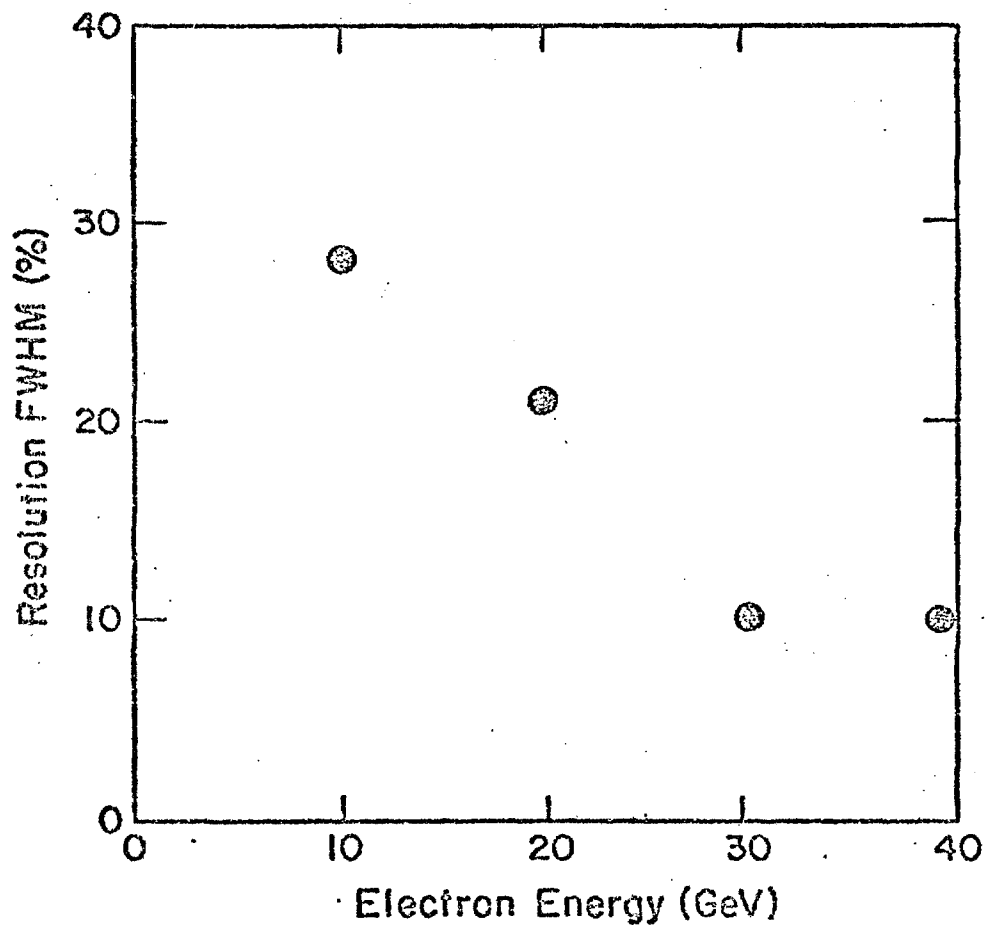


Fig. 9